LAWRENCE
LIVERMORE
NATIONAL
LABORATORY

LLNL-JRNL-660599

Compound specific amino acid 13C patterns in a deep-sea proteinaceous coral: implications for reconstructing detailed 13C records of exported primary production

J. T. Schiff, F. C. Batista, O. A. Sherwood, T. P. Guilderson, T. M. Hill, A. C. Ravelo, K. W. McMahon, M. D. McCarthy

September 18, 2014

Marine Chemistry

Disclaimer

Compound specific amino acid $\delta^{13}C$ patterns in a deep-sea proteinaceous coral: implications for reconstructing detailed $\delta^{13}C$ records of exported primary production

For submission to *Marine Chemistry*

John T. Schiff,[1*] Fabian C. Batista[1], Owen A. Sherwood,[1,2] Thomas P. Guilderson,[1,3] Tessa M. Hill,[4, 5] Ana C. Ravelo,[1] Kelton W. McMahon[1] and Matthew D. McCarthy[1*]

** Corresponding Authors; to whom correspondence should be addressed.*

[1]University of California, Santa Cruz
Department of Ocean Sciences
1156 High Street
Santa Cruz, CA 95064
831-428-3959
(jotschiff@gmail.com)

[2]Institute of Arctic and Alpine Research
University of Colorado, Boulder
1560 30th Street
Boulder, CO 80303

[3]Center for Accelerator Mass Spectrometry
Lawrence Livermore National Laboratory
7000 East Ave
Livermore, CA 94550

[4]University of California, Davis
Department of Earth & Planetary Sciences
One Shields Avenue
Davis, CA 95616

[5]Bodega Marine Laboratory.
2099 Westside Rd,
Bodega Bay, CA 94923

ABSTRACT

Deep-sea proteinaceous corals represent high-resolution paleoarchives, extending biogeochemical time series far beyond recent instrumental data. While recent studies have applied compound specific amino acid $\delta^{15}N$ ($\delta^{15}N$-AA) measurements of their organic skeletal layers to investigate Holocene nitrogen cycling, potential applications of amino acid $\delta^{13}C$ ($\delta^{13}C$-AA) in proteinaceous corals have not yet been examined. Here we developed $\delta^{13}C$-AA analysis in deep-sea bamboo coral (*Isidella* sp.) from the Monterey Canyon to reconstruct exported primary production over an ~80 year record. Preserved deep-sea coral essential amino acid $\delta^{13}C$-AA patterns ($\delta^{13}C$-EAA) closely matched those expected from natural and cultured phytoplankton, supporting the hypothesis that deep-sea coral $\delta^{13}C$-EAA values represent unaltered signatures of exported primary production sources. The coral bulk $\delta^{13}C$ record showed cyclic 0.5‰ variations over the last century, with a shift to lower $\delta^{13}C$ values in the early 1960s. Variations in coral $\delta^{13}C$-EAA values closely followed bulk $\delta^{13}C$ signatures, although both the range and the magnitude of change in the bulk $\delta^{13}C$ record were highly attenuated compared to the $\delta^{13}C$-EAA record. Our results indicate that $\delta^{13}C$-EAA in proteinaceous corals represent a new, direct proxy for $\delta^{13}C$ in primary production that is more sensitive and accurate than bulk $\delta^{13}C$. To test this idea, we used existing phytoplankton $\delta^{13}C$-AA data to calculate an offset between bulk $\delta^{13}C$ and $\delta^{13}C$-EAA. When applied to our data, a reconstructed record of $\delta^{13}C$ values for exported organic matter was consistent with regional phytoplankton dynamics and expected trophic transfer effects, suggesting significant AA resynthesis only in the non-essential AA pool. Together, these results indicate that $\delta^{13}C$-EAA in deep-sea proteinaceous corals provide a powerful new long-term, high resolution tool for investigating variations in exported primary production and biogeochemistry.

1. Introduction

During the last 40 years, stable isotope analysis has proven to be a powerful tool for tracing organic carbon in the geosphere. The $\delta^{13}C$ signature of detrital organic matter has been widely applied to trace carbon sources, such as when comparing terrestrial and marine carbon (e.g., Goni et al., 1997; Meyers, 1994; Meyers, 1997), chemosynthetic biosynthate (e.g., Rau and Hedges, 1979; McCarthy et al., 2011), or relative mixtures of different major biochemical classes (e.g., Roland et al., 2008). Variations in carbon isotopic fractionation during CO_2 uptake have been linked to plankton growth rate, cell size, and pCO_2, such that $\delta^{13}C$ values vary widely in marine microalgae from different latitudes and/or characteristic ocean regions (Goericke & Fry 1994, Rau et al., 1990; Rau et al., 1992; Rau et al. 2001). As a result, $\delta^{13}C$ values for sedimentary organic matter are important paleoceanographic proxies, because variations can provide information about shifts in oceanographic regime, productivity, organic matter source, and pCO_2 over widely varying timescales.

Proteinaceous corals in the orders Alcyonacea, Antipatharia and Zoantharia represent promising new archives for high-resolution paleoceanographic reconstruction (Roark et al., 2005; Sherwood et al., 2005; Williams and Grottoli, 2010; Sherwood et al., 2011; Guilderson et al., 2013; Sherwood et al., 2014). These corals secrete endoskeletons composed of diagenetically resistant, fibrillar protein (e.g., Sherwood et al., 2006). Alcyonacean skeletons are reinforced with carbonate to variable extents. While the skeletal carbonate derives from DIC at depth, radiocarbon evidence indicates that the skeletal protein is synthesized from particulate organic matter (POM) recently exported from surface waters (Griffin and Druffel, 1989; Roark et al., 2005; Roark et al., 2006; Sherwood and Edinger, 2009; Hill et al., 2014). This means that the chemical and isotopic composition of proteinaceous skeletal material reflects an integration of

exported primary production (EPP). These corals deposit laminar growth layers and lifespans range from decades to millennia (e.g., Roark et al., 2009; Sherwood and Edinger, 2009). Together, these factors mean deep-sea corals can provide long-term, high-resolution (annual or even sub-annual) paleooceanographic records that are not possible with sedimentary archives, thus extending biogeochemical time series far beyond the time limits of current instrumental capabilities.

Most geochemical work involving proteinaceous corals has focused on stable isotopic measurements of total ("bulk") skeletal material, as a proxy for changes in surface ocean conditions (e.g., Sherwood et al., 2005; Williams et al., 2007; Sherwood et al., 2009; Williams and Grottoli., 2010a, 2010b). However, bulk isotopic analysis has multiple inherent drawbacks. One of the biggest challenges to interpreting bulk stable isotope data is determining whether changes in a consumer's stable isotope values are due to changes in diet or variability at the base of the food web ($\delta^{13}C_{baseline}$, $\delta^{15}N_{baseline}$), change in trophic position or variability in trophic fractionation ($\Delta^{13}C_{C\text{-}D}$, $\Delta^{15}N_{C\text{-}D}$), or some combination of all of these factors (McMahon et al., 2013). For example, the bulk tissue stable isotope values of deep-sea coral colonies reflect variability in the sources of primary and secondary production contributing to sinking POM. These signatures will be further modified by trophic transfers both during POM export and incorporation of POM into coral biomass. While a relatively modest 1‰ change per trophic transfer ($\Delta\delta^{13}C$) is often assumed (DeNiro and Epstein, 1978), trophic fractionation values can vary widely and are poorly constrained (McMahon et al., 2013). Additionally, while deep-sea corals may be assumed to represent a single trophic transfer from the exported POM they consume, selective feeding or changes in planktonic community structure (induced by environmental change) might also alter the average trophic position between phytoplankton and

exported POM. As a result, bulk tissue $\delta^{13}C$ values in coral skeletal material and polyp tissue are often substantially removed from primary production values: indeed there is biochemical fractionation between the polyp (rich in lipids) and the proteinaceous skeleton (Roark et al., 2009; Sherwood et al., 2008). Together, these factors introduce substantial uncertainty when interpreting bulk $\delta^{13}C$.

Compound specific isotope amino acid analysis (CSI-AA) is a rapidly evolving analytical tool that can resolve much of the uncertainty in bulk isotopic data. $\delta^{15}N$ CSI-AA has now been measured in many different types of organisms in order to analyze trophic dynamics and decouple baseline $\delta^{15}N$ values from food web effects (e.g., McClelland and Montoya, 2002; McClelland and Montoya, 2003; Popp et al., 2007; Sherwood et al., 2011; Sherwood et al., 2014). In contrast, $\delta^{13}C$-AA applications have not been investigated in as much detail. Research to date suggests that $\delta^{13}C$-AA patterns show promise as a tracer for specific C and protein sources within food webs (e.g., Fantle et al., 1999; McMahon et al., 2011a; Larsen et al., 2012; Larsen et al., 2013). However, in paleoceanographic applications, $\delta^{13}C$-AA may also be useful in reducing uncertainty related to tissue offsets and trophic effects. This idea is based on the division between non-essential and essential amino acids (NEAA and EAA, respectively). Generally, the molecular carbon skeletons of EAA cannot be synthesized by higher organisms (e.g., Rawn, 1983), and these structures are not altered during incorporation into biomass (i.e., "salvage" uptake, or direct incorporation of a molecular structure into a consumer). As a result, assuming there are no extensive diagenetic effects, it seems likely that the $\delta^{13}C$-EAA values are not altered during trophic transfer (e.g., O'Brien et al., 2002; McMahon et al., 2010).

In this study, our ultimate goal was to explore the potential for deep-sea coral $\delta^{13}C$-EAA as a new, high-resolution proxy for $\delta^{13}C$ of exported primary production (EPP). We analyzed $\delta^{13}C$-

AA in gorgonin skeletal material from bamboo coral (*Isidella* sp.) collected live in 2007 that recorded approximately 80 years of prior ocean history from the Monterey Canyon. We compared coral δ^{13}C-AA patterns with those known from marine zooplankton and phytoplankton to establish a relationship between coral and primary producer δ^{13}C-AA signatures. We hypothesized that δ^{13}C-EAA in a deep-sea coral should represent an integrated average of EAA from all autotrophic sources. If this is the case, the δ^{13}C-EAA measured in the coral paleoarchive should represent a precise record of exported production that is decoupled from trophic fractionation and tissue-specific offsets that limit the utility of conventional bulk stable isotope analysis. Our development of deep-sea coral CSI-AA will have important implications for extending our understanding of past ocean conditions well beyond the modern instrumental record.

2. Methods

2.1 Sampling

One bamboo coral specimen, T1104-A07, (*Isidella* sp.) was live-collected in 2007 in the Monterey Canyon, Monterey Bay, California at 870 m depth (36°44'39.2280", -122°02'13.9740). Bamboo coral skeletons consist of ~5 – 15 cm long carbonate segments, separated by ~5 – 20 mm thick nodes of proteinaceous gorgonin (Noé et al., 2008). The coral was sectioned and dried at UC Davis, and an ~11 mm thick basal nodal disc was shipped to UC Santa Cruz for isotopic analysis. The skeletal disc was immersed in 10% HCl to dissolve the carbonate from the node, and the remaining node was rinsed in distilled water. Using scalpel and tweezers under a binocular microscope, approx. 0.5 – 1 mm thick peels were separated, following the concentric growth rings, starting from the outer margin of the node and working inward (*see* Sherwood at

148 al., 2009). Sample peels (n = 45) were placed in 5 ml polyethylene vials and re-dried at 50°C for
149 24 hours. Each peel was subsampled for radiocarbon, bulk $\delta^{13}C$, and $\delta^{13}C$-AA analysis.
150
151 *2.2 Radiocarbon analysis*
152 Radiocarbon analysis to construct a coral age model was conducted on eight selected peel
153 subsamples (~700 μg each) at the Center for Accelerator Mass Spectrometry (CAMS) at
154 Lawrence Livermore National Laboratory (LLNL). CO_2 from the coral samples was graphitized
155 after methods outlined in Vogel et al. (1987); method details used at CAMS have also recently
156 been described in more detail by Roark et al. (2006) and Walker et al. (2008). The ^{14}C data were
157 corrected for $\delta^{13}C$ fractionation, and include a matrix-specific background subtraction and are
158 presented in concordance with standard conventions defined by Stuiver and Polach (1977) using
159 the 5568 yr Libby half-life.
160
161 *2.3 Bulk $\delta^{13}C$ analysis*
162 Peel subsamples (n = 45, ~300 μg each) were loaded into tin capsules and analyzed for
163 bulk $\delta^{13}C$ values with a standard dumas (flash) combustion Carlo Erba 1108 elemental analyzer
164 coupled to a ThermoFinningan Delta Plus XP isotope ratio mass spectrometer (EA-IRMS),
165 following standard protocols in the University of California, Santa Cruz Stable Isotope
166 Laboratory (http://es.ucsc.edu/~silab/index.php). We also performed a second, independent
167 sampling from the same peels to assess sampling variability (*See Fig.1, supplementary*
168 *information*). Stable isotope values are reported using standard delta (δ) notation in parts per
169 thousand (‰) using the following equation:
170 $$\delta^{13}C = [(R_{sample}/R_{standard}) - 1] \times 1000 \quad (1)$$

where R is the $^{13}C/^{12}C$ ratio. The reference standard for carbon is Vienna PeeDee Belemnite (VPDB). We split the bulk results into two groups, pre- and post-1960s and used one-way analysis of variance (ANOVA) to test the null hypothesis that there is no statistically significant difference between these two groups. ANOVA was performed in Excel with Data Analysis ToolPak.

2.4 Compound specific $\delta^{13}C$ amino acid analysis

Based on the main features of the bulk $\delta^{13}C$ record, peel subsamples (n = 10, ~10 mg each) were selected for $\delta^{13}C$-AA analysis. Eight peels were analyzed individually and, due to lack of sufficient material in the smallest diameter rings, the four innermost peels were combined into two individual composites. Sample aliquots were hydrolyzed in 6N HCl (110°, 20 hr) and derivatized to isopropyl-TFA esters using established protocols (e.g., Silfer et al., 1991; McCarthy et al., 2013). $\delta^{13}C$-AA measurements were made with a Thermo Trace gas chromatograph (DB-5ms 0.32mm ID x 50m length x 0.25µm film thickness) coupled with a Finnigan Delta Plus XP isotope ratio mass spectrometer (GC-IRMS). Samples were analyzed in triplicate, bracketed by analysis of an in-house AA standard mixture with known $\delta^{13}C$ values. Final amino acid $\delta^{13}C$ values were corrected for added carbon following the approach of Silfer et al (1991). Peak identification and manual baseline correction was performed with Isodat 2.0 software. $\delta^{13}C$ values were determined for twelve AA: the essential amino acid (EAA) group, consisting of Phenylalanine (Phe), Threonine (Thr), Isoleucine (Ile), Leucine (Leu), Valine (Val), and Lysine (Lys); and the non-essential amino acid (NEAA) group, consisting of Aspartic acid + Aspartate (Asx), Glutamic Acid + Glutamate (Glx), Proline (Pro), Alanine (Ala), Serine (Ser), and Glycine (Gly). Standard deviation for triplicate injections ranged from 0.0 – 1.8‰; the

194 average standard deviation across the entire data set (i.e., for all AA measured) was 0.3‰ ± 0.3
195 (Table 1). While analytical precision can vary run to run, and is typically also linked strongly to
196 sample type (e.g., McCarthy et al., 2007), such high precision is not unusual for TFAA
197 derivatives in our laboratory when analyzing pure biological materials (e.g., Volkshoori et al.,
198 2014).

199 *2.5 Normalization and CSI-AA pattern comparisons with marine phytoplankton*

200 We compared CSI-AA biosynthetic patterns in samples having different bulk $\delta^{13}C$ values
201 by normalizing the data to the average $\delta^{13}C$ of the EAA group (e.g., Larsen et al., 2012) using the
202 following equation:

203 $$\delta^{13}C\text{-}AA_n = \delta^{13}C\text{-}AA_m - \delta^{13}C\text{-}EAA_{Avg} \qquad (2)$$

204 where $\delta^{13}C\text{-}AA_n$ is the final normalized $\delta^{13}C$ value of a given AA, $\delta^{13}C\text{-}AA_m$ is the measured
205 value for the same AA, and $\delta^{13}C\text{-}EAA_{Avg}$ is the average (mean) $\delta^{13}C$ value for all EAA measured
206 in a given sample. We used this normalization approach to compare $\delta^{13}C$-EAA patterns in our
207 *Isidella* specimen to literature marine algal $\delta^{13}C$-EAA patterns (compiled by Volkshoori et al.,
208 2014), as well as selected zooplankton $\delta^{13}C$-EAA values from McMahon et al. (2011).

209 *2.6 Linear discriminant analysis*

210 To assess the phylogenetic origin of essential amino acids measured in coral tissue, we applied
211 the linear discriminant function analysis (LDA) approach of Larsen et al. (2009; 2012; 2013).
212 This approach uses LDA coupled with a published "training set" of $\delta^{13}C_{EAA}$ data from
213 evolutionarily distinct groups of potential primary producers, including eukaryotic marine
214 microalgae, axenically cultured bacteria, and brown macroalgae (Larsen et al., 2013), in order to
215 predict likely group membership based on measured $\delta^{13}C_{EAA}$ values in coral peels. The LDA

predictive analyses were performed in R version 2.12.1 (R-Development-Core-Team, 2012) using RStudio interface version 0.98.501 and R package MASS (Venables and Ripley, 2002).

3. Results and Discussion

3.1 Coral age, growth rate, and bulk $\delta^{13}C$ record

Eight sample peels were measured for radiocarbon (Fig. 1). The innermost peel had a $\Delta^{14}C$ value of -98 ± 3‰ (peel #39) and the next oldest sample had a value of -76.9 ± 3‰ (peel #21). The value for peel #39 reflects pre-bomb levels of ^{14}C in the water column. The increase in ^{14}C reached a peak value of +52.6 ± 3.3‰ in peel #11, consistent with oceanic uptake of bomb produced radiocarbon beginning in the late 1950s (Mahadevan, 2001; Kerr et al., 2005). Taking 1958 ± 2 as the year in which the ocean began taking up bomb-^{14}C (Mahadevan, 2001; Kerr et al., 2005), we assigned this year to peel number 21 (distance = 6.65 mm). Combined with the year of collection (2007; distance = 0 mm), we defined a strictly linear age model (e.g., Roark et al., 2005; Sherwood and Edinger, 2009). This age model (based on Fig. 1 data) indicates that the *Isidella* record (radius = 10.76 mm) spans ~80 years. The calculated linear growth rate (136 μm yr^{-1}) is consistent with measured bamboo coral growth rates from similarly highly productive environments (Roark et al., 2006; Thresher et al., 2007; Tracey et al., 2007; Sherwood et al., 2009). Overall, this growth rate indicates that each peel represents 1.8 ± 1.5 yrs (range <1 yr to 8 yrs).

The average $\delta^{13}C$ for the bulk record (from the primary run only, values plotted in Fig. 2) was –16.01 ± 0.2‰. The $\delta^{13}C$ values from a duplicate sub-sampling of the same peels also showed excellent agreement, demonstrating the reproducibility of this peel-based sampling approach (*Fig. 1, supplementary information*). Most time intervals in the record indicate

238 relatively similar $\delta^{13}C$ value in Monterey Bay, with sample-to-sample variability typically <
239 ~0.5‰. However, a significant shift to lower $\delta^{13}C$ values appears to have occurred in the early
240 1960s. While there are also some excursions to lower values in the earlier part of the record
241 (which would require additional specimens to verify), values between the 1930s and the 1960s
242 are generally higher than those from the 1970's to present (Fig. 2). Pre-1960s $\delta^{13}C$ values
243 averaged -16.2 ± 0.27‰, while post-1964 $\delta^{13}C$ averaged -15.9 ± 0.15‰ (groups are significantly
244 different at 95% confidence via one-way ANOVA; $p = 0.004$). While the average offset between
245 these periods does not appear large, there are consistently lower bulk $\delta^{13}C$ values after the mid-
246 1960s (without the larger variation seen in the pre-1960s data), which continue to the end of the
247 record (2007). Because, as noted above (Fig. 1), the chronology of the $\Delta^{14}C$-based record is best
248 constrained around 1960, the timing of this shift in $\delta^{13}C$ values seems very likely to be in the
249 early to mid 1960s.

250 Bulk isotope records are a work-horse of the paleoceanographic community used to
251 explore carbon/biogeochemistry dynamics from the near-instrumental to deep-time. Bulk
252 proteinaceous deep-sea coral records can be generated with small (~ 300 μg) samples quickly
253 and with relative ease compared with the sample size, preparation, and analytical requirements of
254 compound-specific isotope analysis. With regards to this study, the bulk records serve two
255 important functions: the first is to characterize isotopic variability at high (approximately annual)
256 temporal resolution over the length of the available record. The second is to identify optimal time
257 periods in the record where measurement of $\delta^{13}C$-AA will yield the most amount of information
258 about ecosystem change, since currently $\delta^{13}C$-AA cannot be sampled at the same temporal
259 (mass) resolution as that of bulk $\delta^{13}C$.

The reconstruction of specific paleoceanographic trends is not the main goal of this study and in general one should not make large a regional interpretation from a single specimen. However, previous work on bulk isotope records from deep-sea proteinaceous corals haves shown that bulk $\delta^{13}C$ records in particular are typically reproducible between specimens in similar locations, and can provide highly valuable records of broad ecosystem change (Sherwood et al., 2005; Williams et al., 2007, 2010a; Hill et al., 2014). Therefore, the bulk record from our specimen can at least provide a preliminary view of approximately centennial $\delta^{13}C$ trends in primary production in Monterey Bay. In general, the bulk $\delta^{13}C$ record suggests that $\delta^{13}C$ of EPP in Monterey Bay has remained relatively stable over much of the last century. While the overall downward trend in $\delta^{13}C_{bulk}$ appears to be consistent with the oceanic uptake of fossil fuel derived CO_2 (i.e., the Suess effect), the magnitude of this change is less than what has been observed in other areas of the ocean (e.g., Keeling, 1979; Quay and Stutsman, 2003; Swart et al., 2010). Superimposed on this overall trend, there are clear but also relatively minor fluctuations in $\delta^{13}C$ on the order of 0.5‰ (i.e., multiple excursions in Fig. 2, each data point representing ~2 yr integrations). Very close to 1964, however, the data suggests a monotonic shift may have occurred toward more negative $\delta^{13}C$ values. This implies that a state shift in the Monterey Bay biogeochemical carbon cycling may have occurred around this time. Because the Monterey Bay is a highly productive region that is sensitive to numerous climatic and oceanographic processes, there could be multiple explanations for this apparent excursion. A more detailed exploration of this possible shift, including potential explanations, is beyond the scope of this paper, and will require collection and analysis of additional regional coral specimens. We suggest this Monterey Bay bulk $\delta^{13}C$ record will serve as a valuable reference as additional corals become available which together can provide more detailed interpretation.

3.2 Compound specific amino acid $\delta^{13}C$ values

The CSI-AA $\delta^{13}C$ results for replicate coral subsamples produced similar patterns and values (Fig. 3). The average bulk $\delta^{13}C$ for the subsamples used for CSI-AA was -15.93 ± 0.3‰, and the average total hydrolyzable amino acid $\delta^{13}C$ value (the molar percent weighted $\delta^{13}C$ value; $\delta^{13}C_{THAA}$) across the same samples was within the 1σ error ($\delta^{13}C_{THAA}$ = -15.88 ± 1.5‰). Since the gorgonin is dominated by protein, the close match between these values indicates that $\delta^{13}C$-AA values are accurately measuring all major amino acids in the gorgonin skeleton. This also indicates for the first time that $\delta^{13}C$-AA values can provide a molecular-level understanding of variation in gorgonin bulk $\delta^{13}C$ values.

When considering the *Isidella* $\delta^{13}C$-AA results with respect to other heterotrophic organisms, both the range and offsets of individual AA $\delta^{13}C$ values conform to expectations. The overall range between individual AA $\delta^{13}C$ values is large (> 40‰), consistent with previous studies (McMahon et al., 2010). The EAA had depleted $\delta^{13}C$ values (average -21.16 ± 0.9‰) relative to the mean bulk $\delta^{13}C$ value while the average NEAA $\delta^{13}C$ value was much less depleted (-11.74 ± 1.6‰). This is consistent with ^{13}C in NEAA being further enriched during trophic transfer (Vizzini and Mazzola, 2003; France and Peters, 2011). Therefore, the overall $\delta^{13}C$-AA patterns in our *Isidella* specimen are consistent with the hypothesis that EAA directly reflect primary production sources, although we note that value comparisons alone cannot conclusively make this linkage.

3.3 Comparison to phytoplankton $\delta^{13}C$-AA patterns

We compared the $\delta^{13}C$-AA patterns in *Isidella* to $\delta^{13}C$-AA patterns in marine algae and zooplankton to test the underlying hypothesis that EAA $\delta^{13}C$ values derive directly from primary

production sources, without influence from trophic transfers. Previous work has indicated that δ^{13}C-AA patterns for different marine plankton sources are very similar (e.g., McCarthy et al., 2004; Chikaraishi et al., 2009), and those patterns are passed on to upper trophic level consumers virtually unmodified (McMahon et al. 2010; McMahon et al., 2011a). After normalizing measured δ^{13}C-EAA values, the resulting pattern should therefore correspond with the marine algal pattern, despite having been transferred through the food web. The δ^{13}C-EAA pattern in the *Isidella* specimen closely matches the expected pattern from published plankton δ^{13}C-AA data (Fig. 4; Vokhshoori et al., 2014) with the exception of Lys, which shows high variability between the two patterns. However, we caution drawing conclusions from Lys δ^{13}C values; Lys is notoriously challenging to accurately analyze (co-elutes with tyrosine and has poor chromatography).

While the overall match between the normalized EAA patterns in the *Isidella* and plankton species seems remarkably close, the patterns for NEAAs is much further apart (Fig. 4). In a heterotroph, NEAA offsets from the autotrophic pattern indicates that resynthesis has occurred, and is generally expected (McMahon et al., 2010; McMahon et al., 2011b). The much greater ranges for NEAA in autotrophic sources is also consistent with the high variability in specific AA (e.g., Ser and Gly; McMahon et al., 2011b). Together, this comparison strongly supports the expectation that δ^{13}C-EAA values are maintained through trophic transfer, while δ^{13}C-NEAA values are subject to potentially extensive heterotrophic alteration (O'Brien et al., 2002; McMahon et al., 2010).

One possible caveat with respect to *Isidella* δ^{13}C-EAA patterns is that EAA and NEAA groupings have not been directly studied in proteinaceous corals. In general, cnidarians are phylogenetically distant from metazoan species that the canonical "essential" and "non-essential"

328 dichotomy is based upon. To our knowledge there have been no direct studies on obligate amino
329 acid synthesis in deep-sea protaineacous corals, although some previous studies have suggested
330 that shallow water hermatypic zooxanthellate scleractinian corals can synthesize EAA to a
331 limited degree (Fitzgerald and Szmant, 1997; and related Wang and Douglas, 1999). However, in
332 these studies the canonically "essential" amino acids were not synthesized to the extent of "non-
333 essential" amino acids. Furthermore, we note that caution is warranted in applying the results of
334 experiments using scleractinian corals and cnidaria that harbor symbiotic bacteria and other
335 microorganisms to azooxanthellate proteinaceous deep-sea corals. While the basis of the EAA
336 group in these corals is an interesting topic for further research, the correspondence between
337 phytoplankton and δ^{13}C-EAA patterns clearly does not suggest any significant EAA resynthesis
338 in *Isidella*.

339 *3.4 Linear discriminant analysis of* δ^{13}C-EAA *sources: autotrophic algae vs. bacteria*

340 One important process that could alter the δ^{13}C-EAA patterns of sinking POM available
341 to deep-sea proteinaceous corals is microbial degradation and reworking during water column
342 transit. It is well know that the large majority of sinking POM exiting the euphotic zone is
343 remineralized during water column transit, resulting in dramatically reduced yields of
344 hydrolyzable amino acids, as well as other major biochemical classes (e.g. Wakeham et al.,
345 1997). However, at the same time sinking particles in general retain relatively "fresh"
346 biogeochemical signatures, as opposed to the often more degraded *suspended* POM pool. For
347 example, previous studies have shown that sinking POM has modern radiocarbon (Δ^{14}C)
348 signatures (e.g., Druffel et al., 1992), solid state NMR data has demonstrated broad non-selective
349 degradation of exported POM reaching the deep ocean in multiple basins (Hedges et al., 2001),
350 and perhaps most directly relevant to this study, prior CSI-AA data has shown that deep ocean

sediments trap material with "fresh" algal patterns, lacking characteristic signatures of microbial degradation (McCarthy et al., 2004; McCarthy et al., 2007). For a highly productive, high sediment-accumulation margin regime with a relatively shallow water column (such as Monterey Bay), one would generally expect sinking particles to be strongly dominated by recently exported surface algal material.

To test this expectation, we applied an isotopic fingerprinting LDA model to our EAA $\delta^{13}C$ values, based on the approach and molecular-isotopic training set in Larsen et al. (2013). The LDA approach is based on evolutionary divergence in EAA $\delta^{13}C$ patterns, and has now been increasingly applied to fingerprint relative phylogenetic sources in a variety of both living and detrital OM pools (e.g., Larsen et al., 2012; Larsen et al., 2013; Vokhshoori et al., 2014). This is a particularly effective approach for separating bacterially synthesized AA from those derived from algal AA (Hannides et al., 2013). The LDA results for the Monterey Bay *Isidella* samples predicted marine microalgae as the most likely source for EAA (probability = 96 ± 3%) for all coral peel samples (Fig. 5). Importantly, none of the coral peel samples showed indication of either bacterial or macroalgal $\delta^{13}C_{EAA}$ patterns, indicating that protein contributions from microbially re-worked detritus were negligible, at least when compared to the microalgal sources. This result corresponds closely with conclusions from the more general pattern comparison discussed above (*section 3.3*), as well as the basic organic geochemical expectations for POM source and flux in this high production margin system. It also further supports the basic assumption that deep-sea proteinaceous corals' primary food source is "fresh" sinking particles (as opposed to potentially far more degraded suspended particles), based on $\Delta^{14}C$ data (Roark et al., 2005; Roark et al., 2006; Sherwood et al., 2005, Sherwood et al., 2009), as well as prior $\delta^{15}N_{AA}$ data (Sherwood et al., 2011; Sherwood et al., 2014).

374 *3.5 $\delta^{13}C$ temporal trends in essential amino acids compared to bulk gorgonin*

375 Based on our hypothesis that surface primary production is the main C source for these
376 corals, the variations in δ^{13}C-EAA would be expected to follow those in *Isidella* bulk δ^{13}C
377 values. However, as noted above, the exact bulk δ^{13}C values could also be substantially
378 decoupled from the original primary production signal, for example due to cumulative food web
379 effects. Therefore, we directly compared the bulk δ^{13}C to the average δ^{13}C-EAA for the samples
380 on which CSI-AA was performed, both in terms of relative variation, δ^{13}C values, and dynamic
381 range (Fig. 6). Due to the high variability in NEAA values (Fig. 4), and also the potential for
382 complex and somewhat unpredictable resynthesis effects noted below, we have focused our
383 direct comparison only the more stable EAA values.

384 Temporal variations in average δ^{13}C-EAA values closely tracked the bulk record (Fig. 6).
385 When including all data points in a regression analysis, $r^2 = 0.3$ and $p = 0.099$; however,
386 removing the earliest data points from peels (i.e., the region most likely to exhibit overlap
387 sampling errors; see *Fig. 1*, and *supplementary information*) produces an improved correlation
388 ($r^2 = 0.6$ and $p = 0.02$). This shows a potential limitation of larger sample requirements for CSI-
389 AA based analysis when working with very small specimens. However, overall, good
390 correspondence is evident for the 1960s excursion, as well as relative shifts occurring later (Fig.
391 6). We note that the overall pattern in both bulk and δ^{13}C-EAA shown in Fig. 6 appears different
392 compared to the entire bulk record, due to containing far fewer data points. However, our goal
393 here was only to compare how relative offsets in bulk and δ^{13}C-EAA track each other, rather than
394 to construct a time series record.

Overall, the similarity between these records confirms that changes in *Isidella* bulk $\delta^{13}C$ values closely follow $\delta^{13}C$ values of EPP. However, at the same time, the substantial offset in the relative *magnitude* of the variations between the bulk and EAA records suggest that either other carbon sources, or the resynthesis of NEAA has strongly muted primary production $\delta^{13}C$ changes recorded in the bulk coral $\delta^{13}C$ record. Because of the close match between reconstructed $\delta^{13}C$-THAA and bulk values noted above (Fig. 3) we hypothesize that resynthesis of NE-AA is the more likely scenario. In heterotrophic consumers, the $\delta^{13}C$ values of NEAAs biosynthesized from glycolytic (e.g. glycine) or Krebs cycle (e.g. glutamate) precursors are not closely related to their respective dietary amino acids, but rather the bulk diet $\delta^{13}C$ value (Howland et al. 2003; Jim et al. 2006; Newsome et al. 2011). As a result, $\delta^{13}C$ variations in the bulk record could become strongly muted compared to those in the average EAA record (Fig. 6, primary vs. secondary axis), due to the averaging effect of NEAA biosynthesis from a bulk carbon pool. The gorgonin skeleton, like most tissues, is comprised mostly of NEAA (~75 mol% NEAA vs. ~25 mol% EAA), consistent with the hypothesis that trophic changes could be responsible for the offset observed. Overall, we suggest that this hypothesis (that NE-AA resynthesis, linked to trophic effects) can dampen bulk $\delta^{13}C$ records in deep proteinaceous corals will be an important topic for future research. If correct, this implies that the *actual* shifts in $\delta^{13}C$ values may be substantially greater than are apparent from bulk $\delta^{13}C$ coral analysis. If correct, this would imply that $\delta^{13}C$-EAA represents both a more accurate and more sensitive indicator of shifts in primary production $\delta^{13}C$ values.

3.6 $\delta^{13}C$ EAA values: A new approach to reconstruct $\delta^{13}C$ of EPP

We show that $\delta^{13}C$-EAA values in paleoarchives provide a powerful new tool to reconstruct the bulk $\delta^{13}C$ values of EPP. A conceptual diagram (Fig. 7) summarizes the

418 relationship between δ^{13}C-EAA and bulk δ^{13}C values in a simplified deep-sea coral food web,
419 showing both issues with bulk analysis, and potential of directly measuring δ^{13}C-EAA. The
420 cartoon indicates the major trophic enrichment factors (TEFs), as well as tissue-specific
421 biosynthetic offsets, that underlie the offset (ε) between δ^{13}C values in primary production and in
422 δ^{13}C of bulk gorgonin. We hypothesized that the substantial ^{13}C enrichment in bulk gorgonin
423 skeletal material observed compared to the expected marine primary production (i.e., ~ δ^{13}C 4 to
424 6‰ greater in gorgonin material vs. likely plankton sources) is due to a series of trophic transfer
425 fractionations between phytoplankton, zooplankton, and the coral polyp (TEF 1, TEF 2). As
426 noted above, bulk δ^{13}C values are elevated with each trophic transfer, however the exact
427 magnitude of each TEF is very difficult to predict. In our cartoon we have used δ^{13}C TEF values
428 of ~1‰ (e.g., Fry and Sherr, 1984), although as noted above, TEF values in practice can be
429 highly variable. Further, the coral's food source (sinking POM) is a mixture of primary and
430 secondary production (with relative proportions varying with exact location), whose proportions
431 could change based on overlying planktonic food web variations. Therefore, the cartoon also
432 describes a third pathway representing the effective simultaneous coral feeding on the
433 phytoplankton portion of sinking POM (TEF 3). Overall, consideration of these contributing
434 factors shows that the effective TEF for a given skeletal band would be almost impossible to
435 predict with any precision, due to the dependence on multiple TEF values and the relative
436 composition of labile material in sinking POM.

437 Finally, due to characteristic compound-class fractionations, we would also expect substantial
438 δ^{13}C offsets between the gorgonin skeleton and the total animal (coral polyp). Protein has
439 heavier δ^{13}C values than other major biochemical compound classes (e.g., Hayes, 2001),
440 implying expected heavier δ^{13}C values for the proteinaceous gorgonin skeleton. However,

441 gorgonin is also a unique structural protein, with an AA composition different than that found in
442 muscle or other tissues (Goodfriend, 1997; Sherwood et al., 2006). As a result, a substantial
443 offset between the structural gorgonin and the polyp tissue ("ε Gorgonin") is also likely.

444 Overall, the conceptual cartoon makes it clear that while trends in bulk $\delta^{13}C$ of gorgonin
445 skeletal material might mirror those in primary production sources, the *actual* $\delta^{13}C$ values of
446 primary production can probably be only very roughly estimated from bulk values, because the
447 exact offsets depend on many variables that are both organism and location specific. The net
448 offset might also change through a coral record, and the effective TEF value is likely linked to
449 changes in POM composition. However, even if bulk TEF factors vary greatly, the EAA pass
450 through trophic levels with little or no change in $\delta^{13}C$ values (O'Brien et al., 2002; McMahon et
451 al., 2010). As a result, $\delta^{13}C$-EAA values in gorgonin should represent a direct record of average
452 $\delta^{13}C$-EAA values from surface ocean primary production sources. If a predictable offset between
453 $\delta^{13}C$-EAA and bulk $\delta^{13}C$ for phytoplankton exists, then this could allow a direct calculation of
454 $\delta^{13}C$ for exported primary production (Fig. 7). This concept is supported by our results presented
455 above (Fig. 4), as well as previous research suggesting similar phytoplankton $\delta^{13}C$-AA patterns
456 (e.g., McCarthy et al., 2004).

457 *3.7 Using $\delta^{13}C$-EAA to reconstruct bulk primary production*

458 We measured $\delta^{13}C$-EAA values from our *Isidella* specimen, together with a compilation
459 of literature phytoplankton $\delta^{13}C$-AA data, to calculate "reconstructed" bulk EPP values for
460 Monterey Bay. This calculation is based on the scheme outlined above (Fig. 7). While marine
461 phytoplankton $\delta^{13}C$-AA data are not yet extensive, we followed the approach of Vokhshoori et al.
462 (2014). These authors showed a strong linear relationship between bulk $\delta^{13}C$ and $\delta^{13}C$-EAA
463 across wide range of plankton species. Using this regression relationship (*see Fig. 2*,

464 *supplementary information*), our measured δ^{13}C-AA yield a mean δ^{13}C value of -19.5 ± 0.8‰ for
465 reconstructed EPP production, across all intervals for which we measured δ^{13}C-AA (Fig. 8). This
466 value is much lighter compared to the corresponding average bulk gorgonin value of -15.9 ±
467 0.3‰, and heavier than the average δ^{13}C-EAA (-21.16 ± 0.9‰). These offsets correspond directly
468 with the expected relationships described above (Fig. 7). Our "reconstructed" primary production
469 (RPP) using this approach mirrors all changes in average EAA presented above, since it is offset
470 by a constant (Fig. 7). All main changes in the primary production δ^{13}C pattern therefore track
471 bulk record features, however with the much greater amplitude of δ^{13}C change indicated by the
472 δ^{13}C-EAA data (Fig. 6).

473 Overall, the RPP δ^{13}C values predicted by this approach correspond well with δ^{13}C values
474 in previous research on phytoplankton production in this region (Rau et al., 2001). As noted
475 above, phytoplankton in coastal upwelling zones typically have heavier δ^{13}C values, in contrast
476 with offshore samples. However, ranges also substantially overlap, and exact values are tied to
477 the ocean processes of specific locations. Rau et al. (2001) found that POC from the Monterey
478 Bay had δ^{13}C values with a general range of -18‰ to -24‰ in the 1990s. While these
479 comparisons cannot address any specific feature of this preliminary record, they do support our
480 hypothesis that reasonable δ^{13}C values for exported primary production can be calculated from
481 δ^{13}C-EAA data.

482 *4.0 Overview and conclusions*

483 We have presented the first δ^{13}C CSI-AA data from a deep-sea proteinaceous coral. Our
484 high-resolution (~2 yr intervals) bulk δ^{13}C record from a nearly century old specimen exhibited
485 ~0.5‰ fluctuations on decadal scales, including an apparent shift to lower δ^{13}C values in the

early 1960s. Overall, measured δ^{13}C-AA patterns indicate excellent preservation of AA isotope values in the gorgonin skeletal material. In particular, the δ^{13}C patterns for the EAA closely matched patterns expected from marine phytoplankton, while NEAA patterns were far more variable, and showed clear evidence for AA resynthesis. This strongly supports the basic hypothesis that δ^{13}C-EAA values derive from surface algal production, without significant isotopic fractionation.

Taken together, our results suggest that δ^{13}C-EAA in deep sea proteinaceous corals constitutes a direct record of δ^{13}C of surface export production, which would be unaffected by variations in plankton trophic structure, POM composition, or likely coral species. The correspondence in timing of δ^{13}C-EAA vs. bulk δ^{13}C change in our *Isidella* is also consistent with a plankton surface source for all AA making up gorgonin skeletal carbon. However, we also observed substantial differences in amplitude of the bulk vs. δ^{13}C-EAA records, most likely linked to resynthesis of NEAA that constitute the majority of the total AA pool. This finding implies that much of the isotopic variability in EPP may be obscured in proteinaceous coral bulk δ^{13}C records, and that δ^{13}C-EAA data may represent both a more accurate and more sensitive record of primary production δ^{13}C changes.

Based on the direct link between the EAA and algal sources, we propose that δ^{13}C-EAA data can be used to calculate δ^{13}C values for average EPP. Our finding that a calibration derived from phytoplankton cultures could recreate expected bulk δ^{13}C values for POM has potentially wide implication in paleoceanographic studies. It suggests that δ^{13}C-EAA measurements may be developed as a new tool for more accurate reconstruction of primary production δ^{13}C records in any archive where proteinaceous material is well preserved. Further, despite our focus on δ^{13}C-

508 EAA values, we note that $\delta^{13}C$ values of the NEAA pool may also carry significant,
509 complementary information. Specifically, because AA resynthesis linked to trophic transfer
510 should occur only in the NEAA pool, we hypothesize that comparing relative change in both
511 groups might provide complementary information about shifts in food web structure over time.
512 Understanding the information potential in NEAA $\delta^{13}C$ in living organisms is now in early stages
513 (e.g., McMahon et al., 2010), however we suggest this area may also have substantial potential in
514 paleoarchives.

515 Finally, we suggest that an important area of future work should be more firmly
516 establishing the offset between $\delta^{13}C$ values in bulk phytoplankton relative to $\delta^{13}C$-EAA, and also
517 investigating if this offset varies among major plankton types. This information will be
518 necessary to more accurately interpret proteinaceous coral $\delta^{13}C$-EAA records in different oceanic
519 regions. The extreme longevity of these organisms suggests that if robust calibrations can be
520 developed, $\delta^{13}C$-EAA measurements may allow extremely high resolution $\delta^{13}C$ records of EPP,
521 potentially spanning the Holocene. The wide-distribution of deep-sea corals further suggests far
522 reaching potential application, to construct detailed records of oceanic baseline isotopic changes.

523 **ACKNOWLEDGEMENTS**

524 We thank Dr. Dyke Andreasen and Dr. Elizabeth Gier at UC Santa Cruz for helping to prepare
525 and/or process samples for bulk and compound specific isotope analysis. We acknowledge D.
526 Clague at MBARI for coral collection via the ROV *Tiburon* (R/V *Western Flyer*). The analytical
527 work was primarily funded by the National Science Foundation (OCE 1061689) and partly by
528 the UCSC Committee on Research. Radiocarbon analyses were performed under the auspices of
529 the U.S. Department of Energy (DE-AC52-07NA27344). Seamount sampling was supported by
530 NOAA West Coast Polar Regions Research Program (NA030AR4300104 to T. M. Hill and H. J.
531 Spero)
532

533

534

535

536

537

538

539

540

541

542

543

544

REFERENCES

Chikaraishi, Y., Ogaw, N.O. and Ohkouchi, N. 2009. Compound-specific nitrogen isotope analysis of amino acids: Implications of aquatic food web studies. Geochimica Et Cosmochimica Acta, 73(13): A219-A219.

DeNiro, M.J. and Epstein, S. 1978. Influence of diet on distribution of carbon isotopes in animals. Geochimica Et Cosmochimica Acta, 42(5): 495-506.

Druffel, E.R.M., Williams, P.M., Bauer, J.E. and Ertel, J.R. 1992. Cycling of dissolved and particulate organic matter in the open ocean. Journal of Geophysical Research-Oceans, 97(C10): 15639-15659.

Fantle, M.S., Dittel, A.I., Schwalm, S.M., Epifanio, C.E. and Fogel, M.L. 1999. A food web analysis of the juvenile blue crab, *Callinectes sapidus*, using stable isotopes in whole animals and individual amino acids. Oecologia, 120(3): 416-426.

Fitzgerald, L.M. and Szmant, A.M. 1997. Biosynthesis of 'essential' amino acids by scleractinian corals. Biochemical Journal, 322: 213-221.

France, R.L. and Peters, R.H. 1997. Ecosystem differences in the trophic enrichment of ^{13}C in aquatic food webs. Canadian Journal of Fisheries and Aquatic Sciences, 54(6): 1255-1258.

Fry, B. and Sherr, E.B. 1984. $\delta^{13}C$ measurements as indicators of carbon flow in marine and freshwater ecosystems. Contributions in Marine Science, 27(SEP): 13-47.

Goericke, R. and Fry, B. 1994. Variations of marine plankton $\delta^{13}C$ with latitude, temperature, and dissolved CO2 in the world ocean. Global Biogeochemical Cycles, 8(1): 85-90.

Goni, M.A., Ruttenberg, K.C. and Eglinton, T.I. 1997. Source and contribution of terrigenous organic carbon to surface sediments in the Gulf of Mexico. Nature, 389(6648): 275-278.

Goodfriend, G.A. 1997. Aspartic acid racemization and amino acid composition of the organic endoskeleton of the deep-water colonial anemone Gerardia: Determination of longevity from kinetic experiments. Geochimica Et Cosmochimica Acta, 61(9): 1931-1939.

Griffin, S. and Druffel, E.R.M. 1989. Sources of carbon to deep-sea corals. Radiocarbon, 31(3): 533-543.

Guilderson, T., McCarthy, M.D., Dunbar, R.B., Englebrecht, A. and Roark, E.B. 2013. Late Holocene variations in Pacific surface circulation and biogeochemistry inferred from proteinaceous deep-sea corals. Biogeosciences, 10(9): 6019-6028.

576 Hannides, C.C.S., Popp, B.N., Choy, C.A. and Drazen, J.C. 2013. Midwater zooplankton and
577 suspended particle dynamics in the North Pacific Subtropical Gyre: a stable isotope
578 perspective. Limnology and Oceanography, 58(6): 1931-1946.

579 Hayes, J.M. 2001. Fractionation of carbon and hydrogen isotopes in biosynthetic processes.
580 Stable Isotope Geochemistry, 43: 225-277.

581 Hedges, J.I. 2001. Evidence for non-selective preservation of organic matter in sinking marine
582 particles. Nature, 409(6822): 801-804.

583 Hill, T.M., Myrvold, C.R., Spero, H.J., Guilderson, T.P. 2014. Evidence for benthic-pelagic food
584 web coupling and carbon export from California margin bamboo coral archives.
585 Biogeosciences, 11: 3845-3854

586 Howland, M.R., Corr, L.T., Young, S.M.M., Jones, V., Jim, S., Van der Merwe, N.J., Mitchell,
587 A.D., Evershed, R.P. 2003. Expression of the dietary isotope signal in the compound-
588 specific $\delta^{13}C$ values of pig bone lipids and amino acids. International Journal of
589 Osteoarchaeology, 13(1-2): 54-65.

590 Jim, S., Jones, V., Ambrose, S.H., Evershed, R.P. 2006. Quantifying dietary macronutrient
591 sources of carbon for bone collagen biosynthesis using natural abundance stable carbon
592 isotope analysis. British Journal of Nutrition, 95(6): 1055-1062.

593 Keeling, C. D. 1979. The Suess Effect: 13Carbon-14Carbon Interrelations. Environment
594 International, 2: 229-300.

595 Kerr, L.A., Andrews, A.H., Munk, K., Coale, K.H., Frantz, B.R., Cailliet, G.M., Brown, T.A.
596 2005. Age validation of quillback rockfish (*Sebastes maliger*) using bomb radiocarbon.
597 Fishery Bulletin, 103(1): 97-107.

598 Larsen, T., Taylor, D.L., Leigh, M.B. and O'Brien, D.M. 2009. Stable isotope fingerprinting: a
599 novel method for identifying plant, fungal, or bacterial origins of amino acids. Ecology,
600 90(12): 3526-3535.

601 Larsen, T., Wooller, M.J., Fogel, M.L. and O'Brien, D.M. 2012. Can amino acid carbon isotope
602 ratios distinguish primary producers in a mangrove ecosystem? Rapid Communications
603 in Mass Spectrometry, 26(13): 1541-1548.

604 Larsen, T. 2013. Tracing carbon sources through aquatic and terrestrial food webs using amino
605 acid stable isotope fingerprinting. PLoS One, 8(9).

606 Mahadevan, A. 2001. An analysis of bomb radiocarbon trends in the Pacific. Marine Chemistry,
607 73(3-4): 273-290.

608 McCarthy, M.D., Benner, R., Lee, C., Hedges, J.I. and Fogel, M.L. 2004. Amino acid carbon
609 isotopic fractionation patterns in oceanic dissolved organic matter: an unaltered

610 photoautotrophic source for dissolved organic nitrogen in the ocean? Marine Chemistry,
611 92(1-4): 123-134.

612 McCarthy, M.D., Benner, R., Lee, C. and Fogel, M.L. 2007. Amino acid nitrogen isotopic
613 fractionation patterns as indicators of heterotrophy in plankton, particulate, and
614 dissolved organic matter. Geochimica Et Cosmochimica Acta, 71(19): 4727-4744.

615 McCarthy, M.D., Beaupre, S.R., Walker, B.D., Voparil, I., Guilderson, T.P., Druffel, E.R.M.
616 2011. Chemosynthetic origin of ^{14}C-depleted dissolved organic matter in a ridge-flank
617 hydrothermal system. Nature Geoscience, 4(1): 32-36.

618 McCarthy, M.D., Lehman, J. and Kudela, R. 2013. Compound-specific amino acid δ^{1}N patterns
619 in marine algae: tracer potential for cyanobacterial vs. eukaryotic organic nitrogen
620 sources in the ocean. Geochimica Et Cosmochimica Acta, 103: 104-120.

621 McClelland, J.W. and Montoya, J.P. 2002. Trophic relationships and the nitrogen isotopic
622 composition of amino acids in plankton. Ecology, 83(8): 2173-2180.

623 McClelland, J.W., Holl, C.M. and Montoya, J.P. 2003. Relating low $\delta^{15}N$ values of zooplankton
624 to N_2-fixation in the tropical North Atlantic: insights provided by stable isotope ratios of
625 amino acids. Deep-Sea Research Part I-Oceanographic Research Papers, 50(7): 849-861.

626 McMahon, K.W., Fogel, M.L., Elsdon, T.S. and Thorrold, S.R. 2010. Carbon isotope
627 fractionation of amino acids in fish muscle reflects biosynthesis and isotopic routing
628 from dietary protein. Journal of Animal Ecology, 79(5): 1132-1141.

629 McMahon, K.W., Berumen, M.L., Mateo, I., Elsdon, T.S. and Thorrold, S.R. 2011a. Carbon
630 isotopes in otolith amino acids identify residency of juvenile snapper (Family:
631 Lutjanidae) in coastal nurseries. Coral Reefs, 30(4): 1135-1145.

632 McMahon, K.W., Fogel, M.L., Johnson, B.J., Houghton, L.A. and Thorrold, S.R. 2011b. A new
633 method to reconstruct fish diet and movement patterns from $\delta^{13}C$ values in otolith amino
634 acids. Canadian Journal of Fisheries and Aquatic Sciences, 68(8): 1330-1340.

635 McMahon, K.W., Hamady, L.L., Thorrold, S.R. and Smith, I.P. 2013. Ocean ecogeochemistry: a
636 review. Oceanography and Marine Biology: an Annual Review, Vol 51, 51: 327-373.

637 Meyers, P.A. 1994. Preservations of elemental and isotopic source identification of sedimentary
638 organic matter. Chemical Geology, 114(3-4): 289-302.

639 Meyers, P.A. 1997. Organic geochemical proxies of paleoceanographic, paleolimnologic, and
640 paleoclimatic processes. Organic Geochemistry, 27(5-6): 213-250.

641 Newsome, S. D., Fogel, M. L., Kelly, L. and del Rio, C. M. 2011. Contributions of direct
642 incorporation from diet and microbial amino acids to protein synthesis in Nile tilapia.
643 Functional Ecology, 25: 1051–1062

644 Noé, S.U., Lembke-Jene, L. and Dullo, W.C. 2008. Varying growth rates in bamboo corals:
645 sclerochronology and radiocarbon dating of a mid-Holocene deep-water gorgonian
646 skeleton (Keratoisis sp.: Octocorallia) from Chatham Rise (New Zealand). Facies, 54(2):
647 151-166.

648 O'Brien, D.M., Fogel, M.L. and Boggs, C.L. 2002. Renewable and nonrenewable resources:
649 Amino acid turnover and allocation to reproduction in lepidoptera. Proceedings of the
650 National Academy of Sciences of the United States of America, 99(7): 4413-4418.

651 Popp, B. N., Graham, B. S., Olson, R. J., Hannides, C. C. S., Lott, M., Lopez-Ibarra, G. &
652 Galvan-Magana, F. 2007. Inisght into the trophic ecology of yellowfin tuna, Thunnus
653 albacares, from compound-specific nitrogen isotope analysis of proteinaceous amino
654 acids. Stable Isotopes as Indicators of Ecological Change, 1: 173-190.

655 Quay, P. D., and Stutsman, J. 2003. Surface layer carbon budget for the subtropical N. Pacific
656 $\delta^{13}C$ constraints at station ALOHA. Deep-Sea Research I, 50, 1045-1061.

657 Rau, G.H. and Hedges, J.I. 1979. Carbon-13 depletion in a hydrothermal vent mussel:
658 suggestion of a chemosynthetic food source. Science, 203(4381): 648-649.

659 Rau, G.H., Teyssie, J.L., Rassoulzadegan, F. and Fowler, S.W. 1990. $^{13}C/^{12}C$ and $^{15}N/^{14}N$
660 variations among size-fractionated marine particules: implications for their origin and
661 trophic relationships. Marine Ecology Progress Series, 59(1-2): 33-38.

662 Rau, G.H., Takahashi, T., Desmarais, D.J., Repeta, D.J. and Martin, J.H. 1992. The relationship
663 between $\delta^{13}C$ or organic matter and $[CO_2(aq)]$ in ocean surface-water: data from a
664 JGOFS site in the northeast Atlantic ocean and a model. Geochimica Et Cosmochimica
665 Acta, 56(3): 1413-1419.

666 Rau, G.H., Chavez, F.P. and Friederich, G.E. 2001. Plankton $^{13}C/^{12}C$ variations in Monterey Bay,
667 California: evidence of non-diffusive inorganic carbon uptake by phytoplankton in an
668 upwelling environment. Deep-Sea Research Part I-Oceanographic Research Papers,
669 48(1): 79-94.

670 Rawn, J.D. 1983. Biochemistry. Harper and Row Publishers, Inc. New York.

671 Reeds, P.J. 2000. Dispensable and indispensable amino acids for humans. Journal of Nutrition,
672 130(7): 1835S-1840S.

673 Risk, M.J., Heikoop, J.M., Snow, M.G. and Beukens, R. 2002. Lifespans and growth patterns of
674 two deep-sea corals: Primnoa resedaeformis and Desmophyllum cristagalli.
675 Hydrobiologia, 471: 125-131.

676 Roark, E. B., Guilderson, T.P., Flood-Page, S., Dunbar, R.B., Ingram, B.L., Fallon, S.J., and
677 McCulloch, M. 2005. Radiocarbon-based ages and growth rates of bamboo corals from
678 the Gulf of Alaska. Geophysical Research Letters, 32(4).

679 Roark, E.B., Guilderson, T.P., Dunbar, R.B. and Ingram, B.L. 2006. Radiocarbon-based ages
680 and growth rates of Hawaiian deep-sea corals. Marine Ecology Progress Series, 327: 1-
681 14.

682 Roark, E.B., Guilderson, T.P., Dunbar, R.B., Fallon, S.J. and Mucciarone, D.A. 2009. Extreme
683 longevity in proteinaceous deep-sea corals. Proceedings of the National Academy of
684 Sciences of the United States of America, 106(13): 5204-5208.

685 Roland, L.A., McCarthy, M.D. and Guilderson, T. 2008. Sources of molecularly uncharacterized
686 organic carbon in sinking particles from three ocean basins: a coupled $\Delta^{14}C$ and $\delta^{13}C$
687 approach. Marine Chemistry, 111(3-4): 199-213.

688 Schelske, C.L. and Hodell, D.A. 1995. Using carbon isotopes of bulk sedimentary organic
689 matter to reconstruct the history of nutrient loading and eutrophication in Lake Erie.
690 Limnology and Oceanography, 40(5): 918-929.

691 Sherwood, O.A., Heikoop, J.M., Scott, D.B., Risk, M.J., Guilderson, T.P., and McKinney, R.A.
692 2005. Stable isotopic composition of deep-sea gorgonian corals Primnoa spp.: a new
693 archive of surface processes. Marine Ecology Progress Series, 301: 135-148.

694 Sherwood, O.A., Scott, D.B. and Risk, M.J. 2006. Late Holocene radiocarbon and aspartic acid
695 racernization dating of deep-sea octocorals. Geochimica Et Cosmochimica Acta, 70(11):
696 2806-2814.

697 Sherwood, O.A., Jamieson, R.E., Edinger, E.N. and Wareham, V.E. 2008. Stable C and N
698 isotopic composition of cold-water corals from the Newfoundland and Labrador
699 continental slope: Examination of trophic, depth and spatial effects. Deep-Sea Research
700 I, 55: 1392-1402.

701 Sherwood, O.A. and Edinger, E.N. 2009. Ages and growth rates of some deep-sea gorgonian
702 and antipatharian corals of Newfoundland and Labrador. Canadian Journal of Fisheries
703 and Aquatic Sciences, 66(1): 142-152.

704 Sherwood, O.A., Thresher, R.E., Fallon, S.J., Davies, D.M. and Trull, T.W. 2009. Multi-century
705 time-series of ^{15}N and ^{14}C in bamboo corals from deep Tasmanian seamounts: evidence
706 for stable oceanographic conditions. Marine Ecology Progress Series, 397: 209-218.

707 Sherwood, O.A., Lehmann, M.F., Schubert, C.J., Scott, D.B. and McCarthy, M.D. 2011.
708 Nutrient regime shift in the western North Atlantic indicated by compound-specific $\delta^{15}N$
709 of deep-sea gorgonian corals. Proceedings of the National Academy of Sciences of the
710 United States of America, 108(3): 1011-1015.

711 Sherwood, O.A., Guilderson, T.P., Batista, F.C., Schiff, J.T. and McCarthy, M.D. 2014.
712 Increasing subtropical North Pacific Ocean nitrogen fixation since the Little Ice Age.
713 Nature, 505(7481): 78-81.

714 Silfer, J.A., Engel, M.H., Macko, S.A. and Jumeau, E.J. 1991. Stable carbon isotope analysis of
715 amino acid enantiomers by conventional isotope ratio mass spectrometry and combined
716 gad chromatography isotope ratio mass spectrometry. Analytical Chemistry, 63(4): 370-
717 374.

718 Stuiver, M. and Polach, H.A. 1977. Discussion: reporting of ^{14}C data. Radiocarbon, 19(3): 355-
719 363.

720 Swart, P. K., Greer, L., Rosenheim, B.E., Moses, C.S., Waite, A.J., Winter, A., Dodge, R.E., and
721 Helmle, K. 2010. The ^{13}C Suess effect in scleractinian corals mirror changes in the
722 anthropogenic CO_2 inventory of the surface oceans. Geophysical Research Letters, 37:
723 L05604

724 Thresher, R.E., MacRae, C.M., Wilson, N.C. and Gurney, R. 2007. Environmental effects on the
725 skeletal composition of deep-water gorgonians (Keratoisis spp.; Isididae). Bulletin of
726 Marine Science, 81(3): 409-422.

727 Tracey, D.M. et al. 2007. Age and growth of two genera of deep-sea bamboo corals (family
728 Isididae) in New Zealand waters. Bulletin of Marine Science, 81(3): 393-408.

729 Venables, W.N. and Ripley, B.D. 2002. Modern applied statistics with S. 4th ed. Springer.

730 Vizzini, S. and Mazzola, A. 2003. Seasonal variations in the stable carbon and nitrogen isotope
731 ratios ($^{13}C/^{12}C$ and $^{15}N/^{14}N$) of primary producers and consumers in a western
732 Mediterranean coastal lagoon. Marine Biology, 142(5): 1009-1018.

733 Vogel, J.S., Southon, J.R. and Nelson, D.E. 1987. Catalyst and binder effects in the use of
734 filamentous graphite for AMS. Nuclear Instruments & Methods in Physics Research
735 Section B-Beam Interactions with Materials and Atoms, 29(1-2): 50-56.

736 Vokhshoori, N.L., Larsen, T, and McCarthy, M.D. 2014. Reconstructing $\delta^{13}C$ isoscapes of
737 phytoplankton production in a coastal upwelling system with amino acid isotope values
738 of littoral mussels. Marine Ecology Progress Series, 504: 59-72.

739 Wakeham, S.G., Lee, C., Hedges, J.I., Hernes, P.J. and Peterson, M.L. 1997. Molecular
740 indicators of diagenetic status in marine organic matter. Geochimica Et Cosmochimica
741 Acta, 61(24): 5363-5369.

742 Walker, B.D. and McCarthy, M.D. 2012. Elemental and isotopic characterization of dissolved
743 and particulate organic matter in a unique California upwelling system: importance of
744 size and composition in the export of labile material. Limnology and Oceanography,
745 57(6): 1757-1774.

746 Walker, B.D., McCarthy, M.D., Fisher, A.T. and Guilderson, T.P. 2008. Dissolved inorganic
747 carbon isotopic composition of low-temperature axial and ridge-flank hydrothermal
748 fluids of the Juan de Fuca Ridge. Marine Chemistry, 108(1-2): 123-136.

749 Wang, J.T. and Douglas, A.E. 1999. Essential amino acid synthesis and nitrogen recycling in an
750 alga-invertebrate symbiosis. Marine Biology, 135(2): 219-222.

751 Williams, B., Risk, M.J., Stone, R., Sinclair, D. and Ghaleb, B. 2007. Oceanographic changes in
752 the North Pacific Ocean over the past century recorded in deep-water gorgonian corals.
753 Marine Ecology Progress Series, 335: 85-94.

754 Williams, B. and Grottoli, A. 2010a. Recent shoaling of the nutricline and thermocline in the
755 western tropical Pacific. Geophysical Research Letters, 37: L22601

756 Williams, B. and Grottoli, A.G. 2010b. Stable nitrogen and carbon isotope ($\delta^{15}N$ and $\delta^{13}C$)
757 variability in shallow tropical Pacific soft coral and black coral taxa and implications for
758 paleoceanographic reconstructions. Geochimica Et Cosmochimica Acta, 74(18): 5280-
759 5288.

TABLES

Table 1. Mean $\delta^{13}C$ values (‰ ± 1σ analytical variation) for measured individual amino acids for peels from *Isidella* specimen (T1104-A07). The estimated year for each sample peel # was derived from the radiocarbon age model (*See Methods*). Essential amino acids*: Phe (Phenylalanie), Thr (threonine), Ile (Isoleucine), Leu (leucine), Val (valine), and Lys (lysine). Non-essential amino acids: Asp (aspartic acid and aspartate), Glu (glutamic acid and glutamate), Pro (proline), Ala (alanine), Ser (serine), and Gly (glycine).

765 **FIGURE CAPTIONS**

766 **Figure 1:** Measured radiocarbon ($\Delta^{14}C$ ‰; y-axis) as a function of sampled distance from the
767 coral edge (mm; x-axis) for *Isidella* coral peels. The maximum value measured (+52.6 ± 3.3‰)
768 corresponds very well with the expected bomb spike value, fixing this sampled interval at 1958 ±
769 2 years in the age model (*see text*). The overall shape of the $\Delta^{14}C$ curve corroborates the
770 expectation that organic matter in the *Isidella* coral originates from surface-derived sinking
771 particulate organic matter.

772

773 **Figure 2.** Bulk $\delta^{13}C$ record for the *Isidella* coral specimen from the Monterey Canyon in central
774 California, with estimated calendar years calculated via a linear ^{14}C age model. Dashed line
775 represents the average bulk $\delta^{13}C$ value.

776

777 **Figure 3.** Compound specific isotope amino acid (CSI-AA) $\delta^{13}C$ values from the *Isidella*
778 specimen across a nearly 80 year record (different symbols represent different years from a linear
779 ^{14}C age model). Amino acids are grouped by their metabolic pathway (Essential or Non-
780 Essential) and their carbon skeleton biosynthetic families (Ar. = Aromatic; Asp. = Aspartic).
781 Dashed line indicates average bulk $\delta^{13}C$ value for all samples (-15.93‰). The average $\delta^{13}C$ value
782 for measured amino acids after adjusting for molar composition (-15.88 ± 1.51‰) was
783 statistically indistinguishable from the bulk value. This indicates that hydrolyzable amino acids
784 represent essentially all organic carbon in the skeletal material.

785

786 **Figure 4.** A comparison of amino acid $\delta^{13}C$ values, normalized to mean essential amino acid
787 (EAA) $\delta^{13}C$ value ($\delta^{13}C_{\text{Normalized}} = \delta^{13}C_{AA}$ - Avg. $\delta^{13}C_{EAA}$), between *Isidella* and literature data

for plankton. The strong similarity of normalized EAA patterns between *Isidella* (open diamonds) and phytoplankton (grey diamonds; *supplementary information*) as well as mixed tows of phytoplankton and zooplankton together (black diamonds; *supplementary information*) confirms that EAA patterns are passed on to upper trophic level consumers virtually unmodified. In contrast, much poorer correspondence between normalized non-essential amino acid (NEAA) patterns for phytoplankton compared to *Isidella* indicates significant resynthesis. For zooplankton and phytoplankton, error bars are ± 1σ across the chosen data sets and for *Isidella* the error bars are ± 1σ across peels. Note that because substantial resynthesis and fractionation is expected for NEAAs with trophic transfer, only pure phytoplankton data are shown for NEAAs.

Figure 5. Linear discriminant phylogenetic source analysis based on essential amino acid (EAA) $\delta^{13}C$ values in *Isidella* . First two linear discriminants are plotted, based on $\delta^{13}C$ values of five essential amino acids (EAA: Ile, Leu, Phe, Thr, Val). Training set data for three categorical variables, marine microalgae (filled triangles, n = 16), bacteria (gray squares, n = 12), and marine macroalgae (open diamonds, n = 12) are from Larsen et al. (2013). The training data set is used to predict the biosynthetic origins of EAAs among coral peel samples (solid X, n = 10). All coral samples classified as microalgae, with an average of 96% probability.

Figure 6. Average essential amino acid values ($\delta^{13}C$-EAA) of *Isidella* coral peels (solid line, left y-axis) compared to the bulk $\delta^{13}C$ record in from those sample samples (dashed line, right y-axis) across an 80 year time series . The close correspondence of changes in both records shows the direct link between coral bulk $\delta^{13}C$ values and primary production. However, the substantial

offset in dynamic ranges (note different scales on the left and right y axis) suggests that $\delta^{13}C$ variation in exported production has been strongly attenuated in the bulk $\delta^{13}C$ record.

Figure 7. Conceptual diagram of reconstruction of primary production $\delta^{13}C$ values based on measured essential amino acid (EAA) $\delta^{13}C$ in the *Isidella* coral gorgonin skeleton. The illustration indicates relative offsets between EAA and bulk $\delta^{13}C$ values (ε), trophic discrimination factors (TEF) associated with trophic transfer in a simplified deep coral food web. The measured bulk $\delta^{13}C$ value (open diamond) of gorgonin skeletal material ("Gorgonin skeleton") can only be related back to initial primary production through a series of poorly constrained bulk fractionation changes. These include changes related to direct trophic transfers, complicated by variable fraction of primary versus secondary production in labile sinking POM (TEF 1 vs. TEF 2 + 3), as well as tissue specific (ε Gorgonin) biosynthetic $\delta^{13}C$ offsets. In contrast, $\delta^{13}C$-EAA values (black diamonds) are constant through trophic transfer.

Figure 8. A record of bulk $\delta^{13}C$ reconstructed primary production ($\delta^{13}C_{RPP}$) compared to bulk $\delta^{13}C$ for *Isidella* sp. gorgonin (Bulk gorgonin). The $\delta^{13}C_{RPP}$ is derived from measured average essential amino acid $\delta^{13}C$-EAA values, and is based on the offset (ε) between plankton bulk $\delta^{13}C$ and $\delta^{13}C$-EAA, which is assumed as a constant (indicated by arrow). The offset was calculated using a published linear regression relationship, as described in the text. While pattern of change is similar for all records, estimated primary production $\delta^{13}C$ values are substantially depleted relative to gorgonin skeleton, consistent with the mechanisms outlined in Figure 7.

832 **FIGURES**

833 Figure 1.

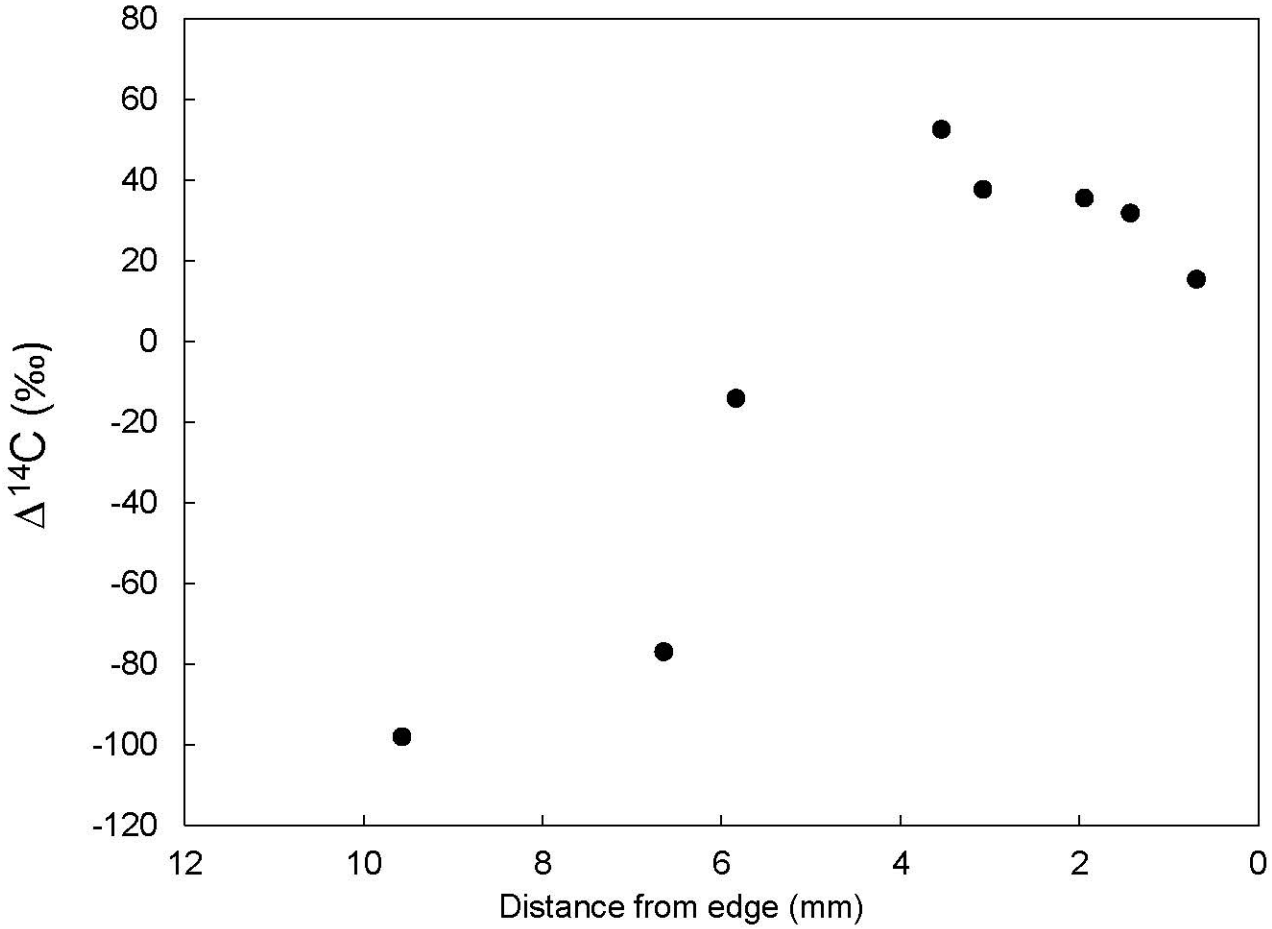

834

835

836

837

838

839

840

841

842

843 Figure 2.

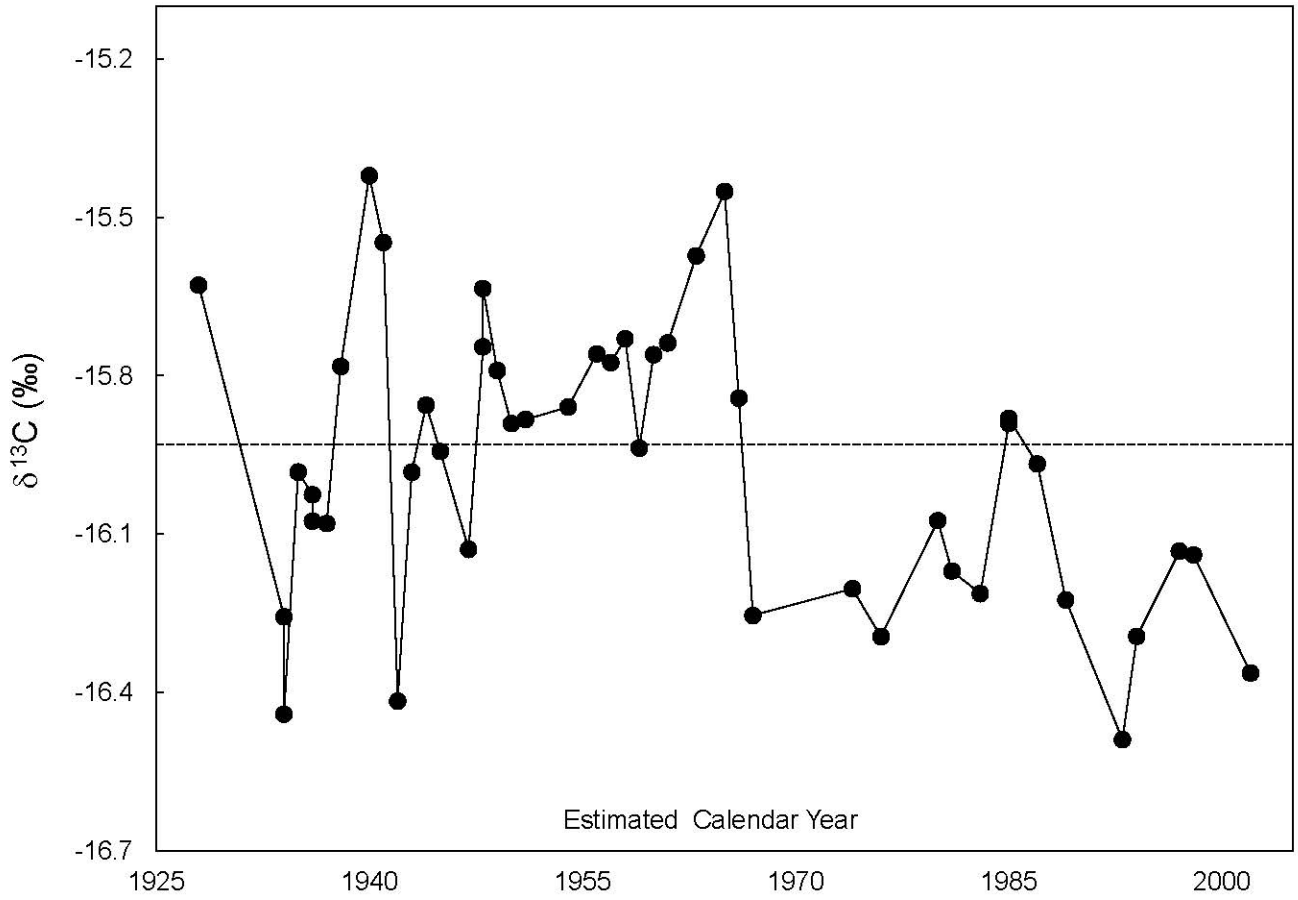

844

845

846

847

848

Figure 3.

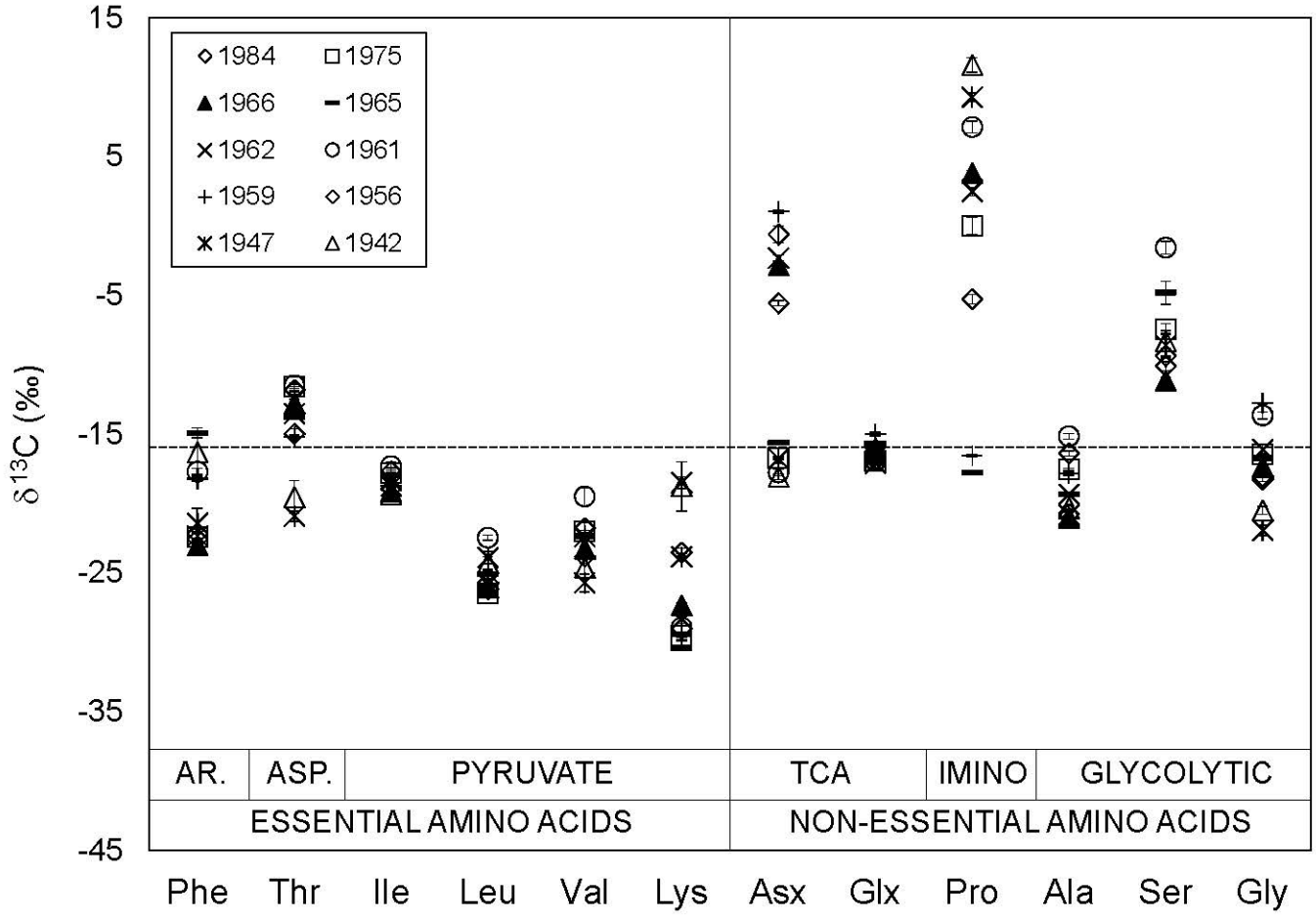
15
5
-5
-15
-25
-35
-45
δ13C (‰)
1984
1975
1966
1965
1962
1961
1959
1956
1947
1942
AR.
ASP.
PYRUVATE
TCA
IMINO
GLYCOLYTIC
ESSENTIAL AMINO ACIDS
NON-ESSENTIAL AMINO ACIDS
Phe
Thr
Ile
Leu
Val
Lys
Asx
Glx
Pro
Ala
Ser
Gly

862

863

864

865

866

867

868 Figure 4.

869

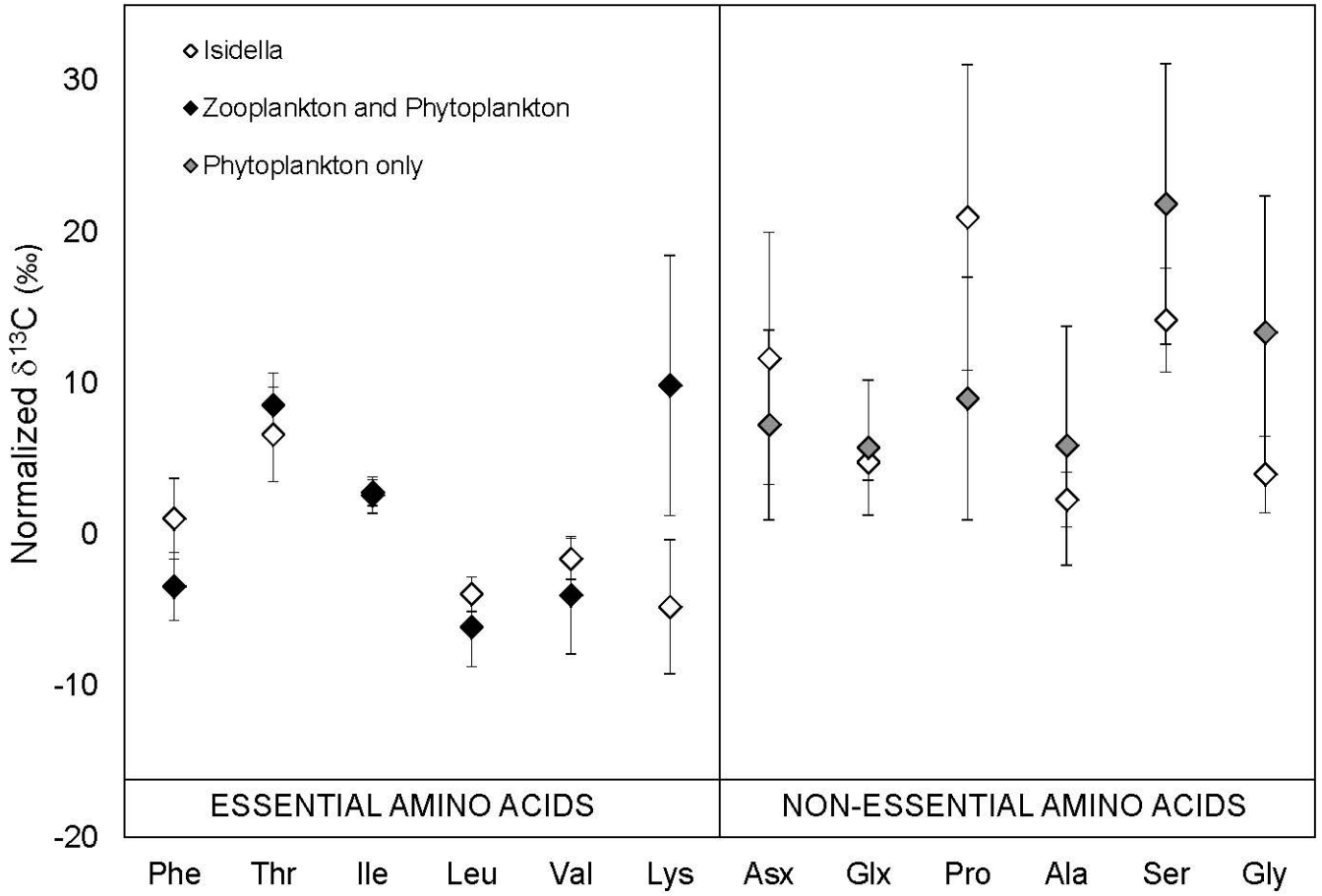

870

871

872

873

874

Figure 5.

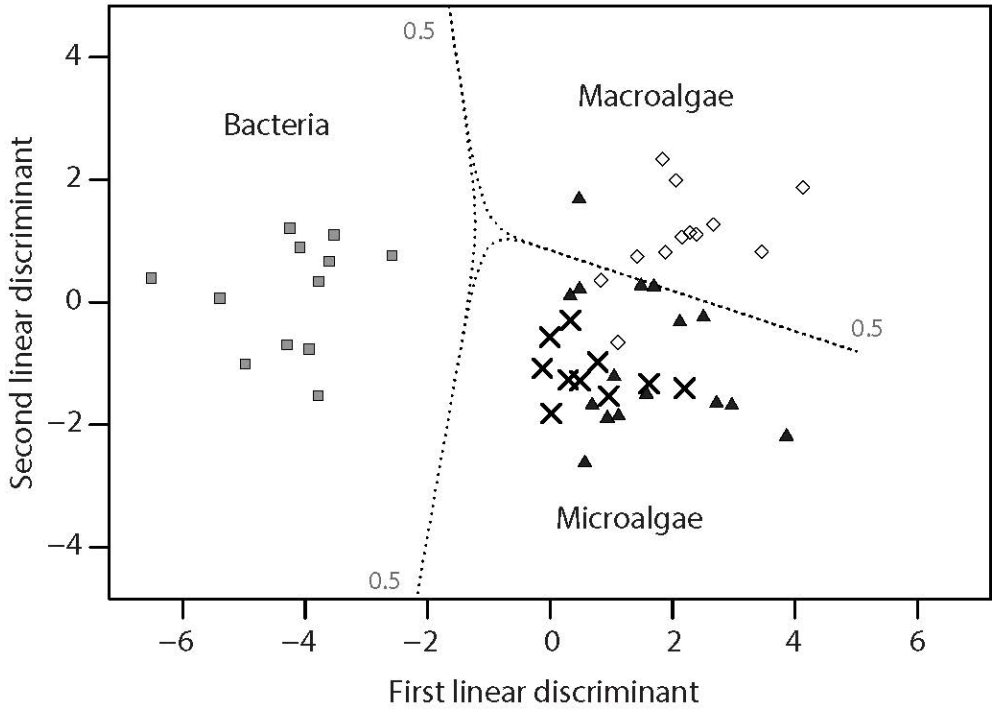
0.5
Macroalgae
Bacteria
0.5
Second linear discriminant
4
2
0
−2
−4
Microalgae
0.5
−6
−4
−2
0
2
4
6
First linear discriminant

883

884

885

886

887

888

889

890

891

892

893

894

895 Figure 6.

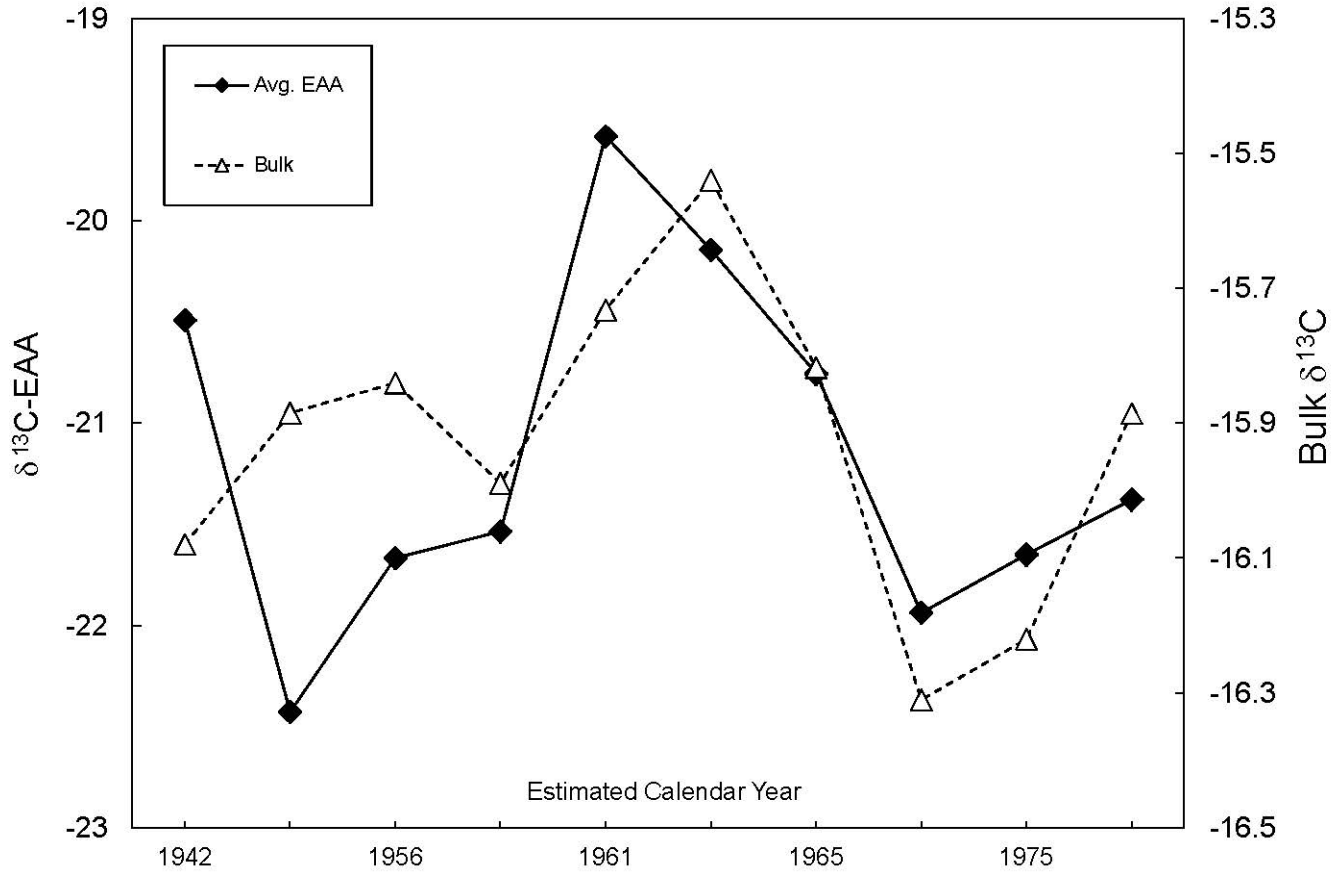
Avg. EAA
Bulk
δ 13C-EAA
Bulk δ 13C
Estimated Calendar Year
-19
-20
-21
-22
-23
-15.3
-15.5
-15.7
-15.9
-16.1
-16.3
-16.5
1942
1956
1961
1965
1975

902

903

904

905

906

907

908 Figure 7.

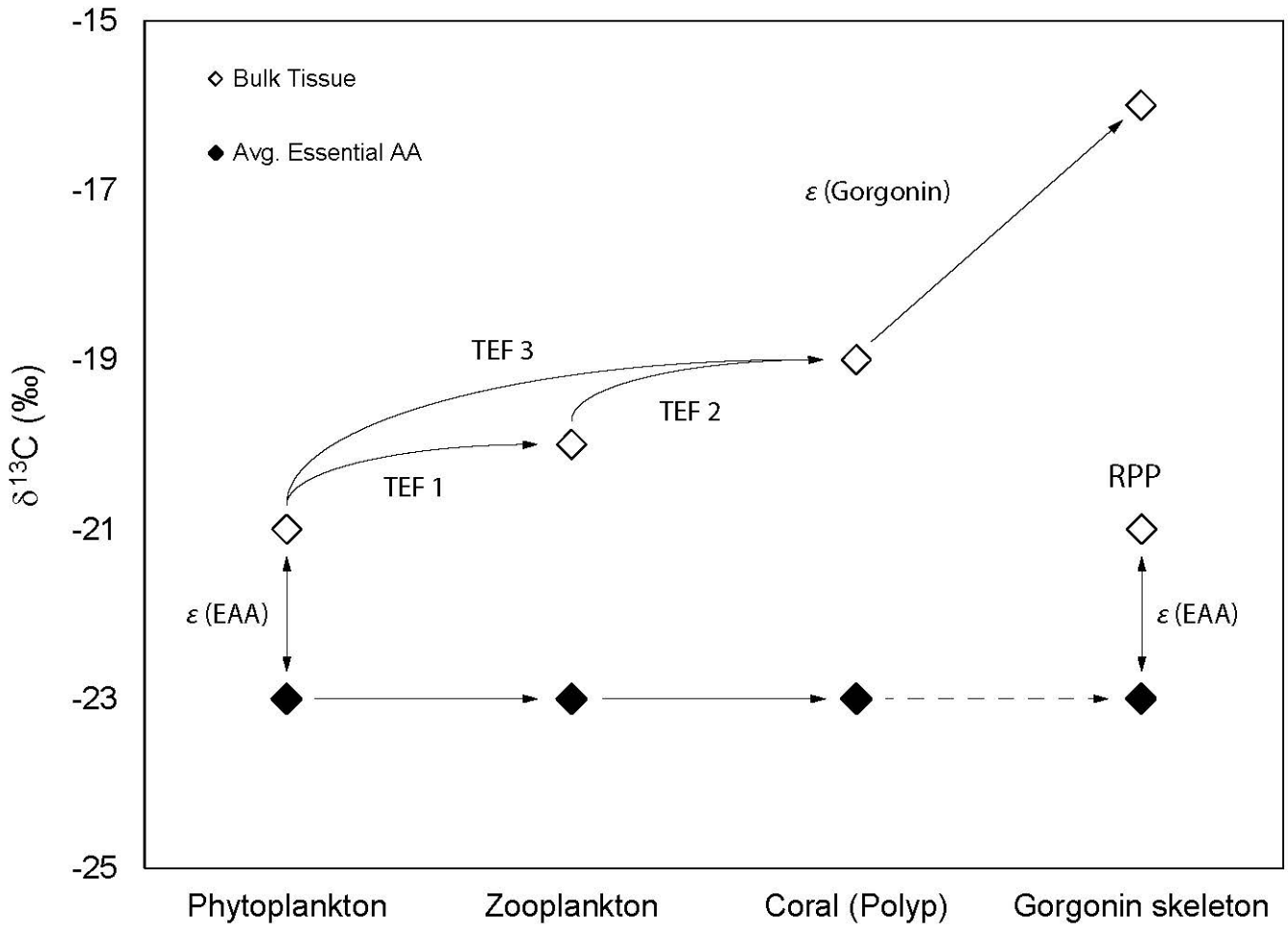

909

910

911

912

913

914

915

916

917

918

919 Figure 8.

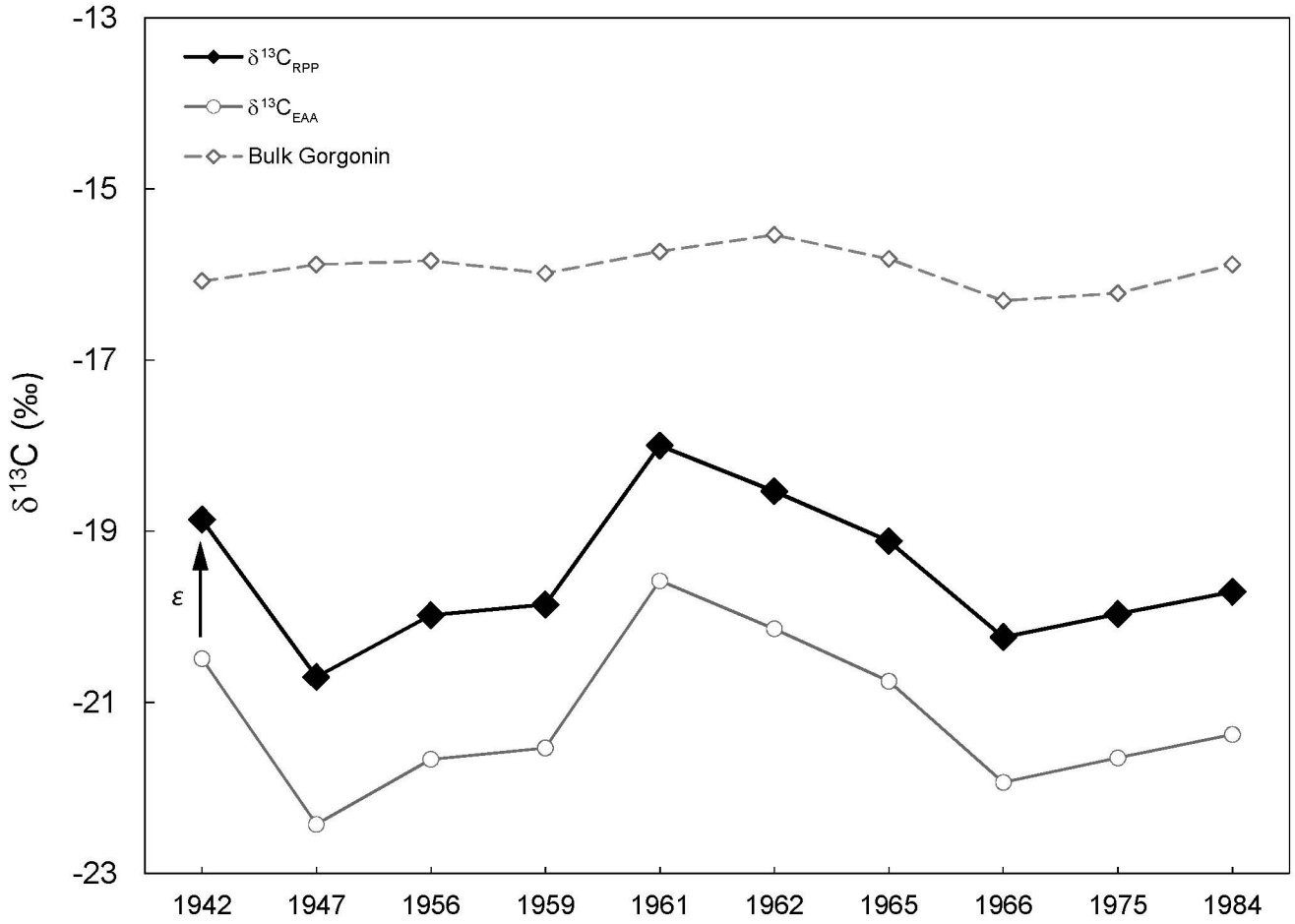
-13
-15
-17
-19
-21
-23
δ13C (‰)
δ13CRPP
δ13CEAA
Bulk Gorgonin
ε
1942
1947
1956
1959
1961
1962
1965
1966
1975
1984

SUPPLEMENTARY INFORMATION

Supplementary Table 1. Mean $\delta^{13}C$ values of bulk and compound-specific amino acids in a range of cosmopolitan eukaryotic photosynthetic species, as compiled by Vokhshoori et al. (2014). Values reported are the mean values reported in respective publications. Data sources: "Larsen" indicates Larsen et al. (2013) and "McCarthy" indicates McCarthy et al. (2013).

			Essential Amino Acids						Non-Essential Amino Acids					
Sample	**Source**	**Bulk**	**Phe**	**Thr**	**Ile**	**Leu**	**Val**	**Lys**	**Asp**	**Glu**	**Pro**	**Ala**	**Ser**	**Gly**
Achnanthes brevipes	Larsen	-12.8	-18.1	-2.7	-10.2	-17.3	-13.8	-8.8	-11.1	-11.4	N/A	-9.7	N/A	-11.2
Amphora coffaeiformis	Larsen	-10.5	-19.6	-2.0	-11.5	-18.7	-16.8	-11.1	-9.1	-7.5	N/A	-7.4	N/A	-12.0
Melosira varians	Larsen	-14.6	-20.6	-7.0	-16.5	-22.1	-19.7	-15.8	-16.2	-12.2	N/A	-10.3	N/A	-12.3
Phaeodactylum tricornutum	Larsen	-19.4	-23.8	-10.8	-16.1	-25.5	-22.9	-15.2	-17.7	-18.9	N/A	-16.0	N/A	-12.2
Stauroneis constricta	Larsen	-9.1	-16.0	-4.6	-10.4	-19.3	-15.5	-8.5	-6.6	-7.4	N/A	-1.3	N/A	5.5
Amphidinium carterea	McCarthy	-23.7	-29.1	-9.6	-22.1	-34.6	-27.7	-18.7	-10.7	-20.0	-24.0	-21.1	-6.1	-8.0
Pseudo-nitzchia	McCarthy	-28.4	-35.0	-24.0	-29.9	-43.3	-33.0	-26.2	-28.9	-30.0	-24.5	-18.6	-13.9	-25.9
Dinoflaggelate sp.	McCarthy	-19.1	-24.7	-8.7	-16.9	-30.7	-22.0	-17.7	-10.6	-11.9	-20.1	-17.7	-1.6	-5.1

Supplementary Figure 1. The first bulk $\delta^{13}C$ run of gorgonin skeletal material in *Isidella* (T1104-A07) superimposed with the second bulk $\delta^{13}C$ run (n = 42) using subsamples (not replicates) of the same individual peels, except for peels 40, 41 and 45 due to lack of material. The generally excellent agreement between records demonstrates reproducibility *within* peels, as previously shown (Sherwood et al., 2005). Offsets between the two bulk records early in the record may be attributed to progressively smaller peel widths closer to the core, allowing for overlap between adjacent peels, resulting in the time offsets observed in the duplicate records.

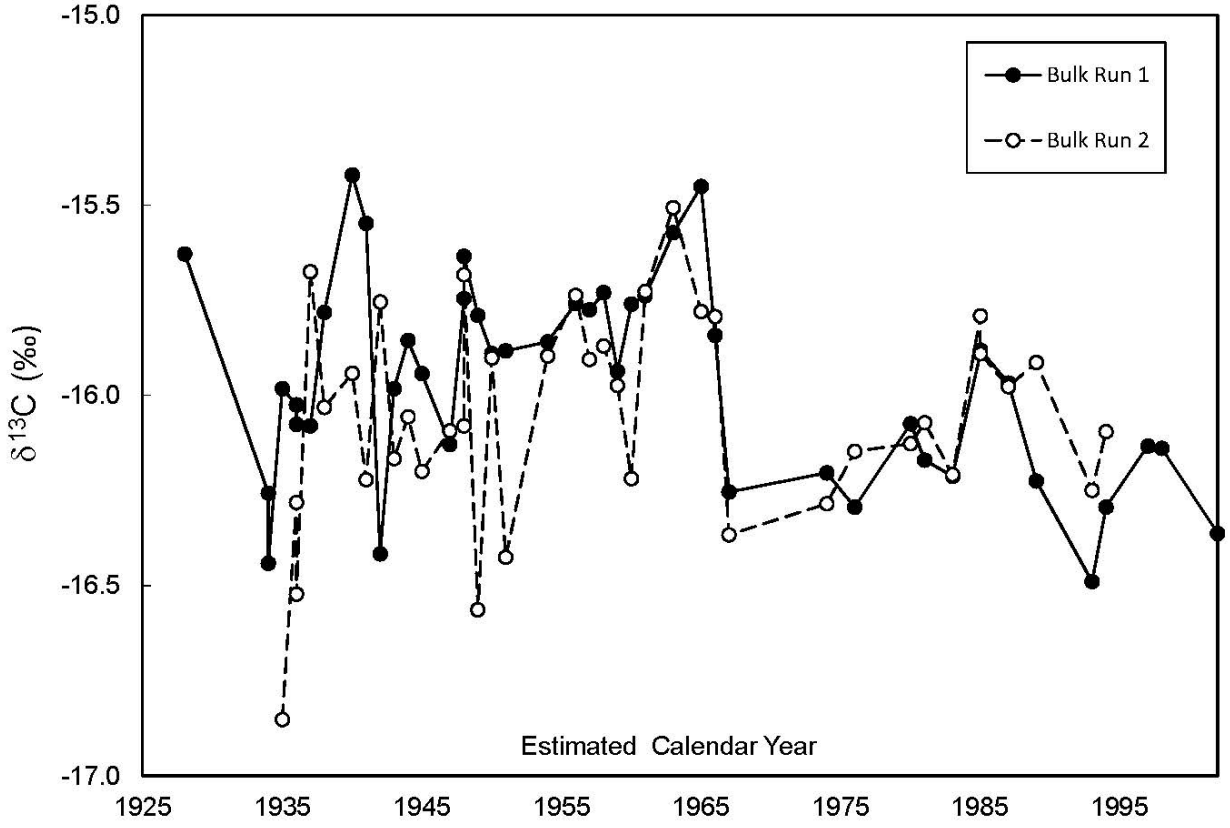

Supplementary Figure 2. The relationship between bulk $\delta^{13}C$ vs. average EAA $\delta^{13}C$ in a modified set of compiled phytoplankton data (n = 8) from Vokhshoori et al. (2014). The $r^2 = 0.93$ indicates a strong correlation and is nearly the same as in Vokhshoori et al. (2014) despite using fewer phytoplankton samples. For our study we removed the prokaryotic cyanobacteria and used only diatom and dinoflagellate species from the compiled set.